Universidade de Aveiro Departamento de Química
2008

Madhu Phani Namburi

Studies on polymer/ carbon based nanoparticles.

Estudos sobre compósitos do tipo polímero/ nanoparticulas de carbono

Universidade de Aveiro Departamento de Química
2008

Madhu Phani Namburi

Studies on polymer/ carbon based nanoparticles.

Estudos sobre compósitos do tipo polímero/ nanoparticulas de carbono

Dissertação apresentada à Universidade de Aveiro para cumprimento dos requisitos necessários à obtenção do grau de Mestre em Engenharia e Ciência dos Materiais, realizada sob a orientação científica da Dra. Ana Barros Timmons, Professora Auxiliar do Departamento de Química da Universidade de Aveiro e do, Professor Auxiliar Lars Rosgaard Jensen do Departamento de Mecânica da Universidade de Aalborg, Dinamarca.

"The important thing in science is not so much to obtain new facts as to discover new ways of thinking about them"

Sir. William Bragg

o júri

presidente

Doutor Dmitry Victorovitch Evtyugin
Professor associado, com agregação da Universidade de Aveiro

Doutora Maria da Conceição de Jesus Rego Paiva
Professora auxiliar da Universidade do Minho

Doutora Ana Margarida Madeira Viegas de Barros Timmons
Professora auxiliar da Universidade de Aveiro

Professor. Lars Rosgaard Jensen
Professor da Universidade de Aalborg

Acknowledgments
Agradecimentos

This present report has been submitted in partial fulfillment of the requirements for the European Masters in Materials Science.

This thesis marks the acme of my masters program at UA and AAU universities, and in this occasion I would like to thank all people who inspired, encouraged and supported me for its successful completion.

There are many people that must be acknowledged for their technical and moral support that led to the completion of this work. Initially I wish to express my deepest gratitude and thanks to my advisor Professor Ana Barros Timmons for giving me the opportunity to work under her guidance and for her valuable advice, guidance, patience and encouragement the completion of this thesis work.

I wish to extend my heartfelt thanks to Professor Lars Rosgaard Jensen for his sound advice and careful guidance at AAU.

I would also like to thank those who agreed to be interviewed, for, without your time and cooperation, this project would not have been possible.

I want to thank my EMMS colleagues for providing me a good support at the time of work and discussion.

In addition, I would like thank the technical support of Chemistry and Ceramic Departments for their assistance and efforts. I would also like to thank all of my EMMS colleagues for many inspiring discussions.

Many thanks to the European Union for the financial support through the Erasmus Mundus Programme.

Finally, I thank my parents for instilling in me confidence and a drive for pursuing my Masters.

To each of the above, I extend my deepest appreciation.

Sincerely

Palavras-chave

Nanotubos de carbono, fibras de carbono, modificação química de superficies, ATRP, compósitos, resinas epoxi, tensão de corte interfacial.

Resumo

A utilização de estruturas à base de carbono (CNT, CNF e CF por exemplo) na preparação de compósitos de matriz polimérica tem despertado bastante interesse tanto no que concerne as suas propriedades como as potenciais aplicações.

A adição deste tipo de cargas em matrizes poliméricas por vezes não provoca qualquer alteração nas propriedades no compóstio devido à sua má dispersão. Por esse motivo é geralmente necessário proceder a uma modificação química da superfícice destas cargas.

Neste trabalho são seguidas duas abordagens distintas. Inicialmente estudou-se a modificação química dos MWCNT e posterior polimerização radicalar viva por ATRP a partir da superfície. Seguidamente, utilizou-se o mesmo processo de modificação superficial à CFs e o seu efeito na interface CF/resina epoxi foi estudado.

No primeiro caso os MWCNTs foram oxidados com ácido nitrico. Aos MWCNTs resultantes ancorou-se um diol e posteriormente um iniciador de ATRP. Seguidamente procedeu-se à polimerização de tert-acrilato de butilo a partir da superfície. Os materiais obtidos foram caracterizados através de testes de solubilidade, análise elementar, TEM, SEM e TGA.

As CF, foram também submetidas ao processo de oxidação da superfície e de ancoramento de um diol. As CFs modificadas foram utilizadas na preparação de compósitos CF/resina epoxi e o efeito da modificação química na interface CF/ polímero foi estudado por espcroscopia de Raman e SEM.

No 1º capítulo é feita uma introdução aos CNTs, às CF, à polimerização radicalar viva por ATRP, à preparação de compósitos. No 2º capítulo apresentam-se os resultados obtidos com os MWCNTs.

No 3º capítulo apresentam-se os resultados obtidos com as CF e discute-se o efeito da modificação superficial sobre as propriedades dos compósitos preparados.

O 4º capítulo consiste num resumo das conclusões tiradas nos capítulos anteriores e são feitas algumas sugestões para trabalhos futuros.

Keywords Carbon nanotubes, surface chemical modification, carbon fibers, epoxy resin, composites, interfacial shear stress.

Abstract

In many cases the influence of these reinforcing materials in polymer matrices is not detected due to poor dispersion. So, for the efficient utilization of these reinforcing materials (MWNTs, CF) in the polymer based composites, needs prior functionalization.

In this work two approaches have been studied: initially the surface oxidation & functionalization of MWNTs and polymerization process were studied and explored. Later the same oxidation & functionalization process was applied to CF surface modification and then it's influence on the interface of CF/ epoxy resin was determined.

In the first approach MWNTs were subjected to oxidation with nitric acid and submitted to the incorporation of a diol spacer. Then they are subjected ATR polymerization process using tert-butyl acrylate as monomer. The modified materials were characterized by solubility tests, elemental analysis, TEM, SEM and thermo gravimetric analysis.

In the next part CF were subjected to same oxidation and diol functionalization process then they are used to produce CF/epoxy resin composites and studies are done on the effect of surface modification on the interface of CF and epoxy matrix. Tensile test in situ Laser Raman Spectroscopy was used to determine the interfacial behavior and properties. Surface modified CF was characterized using LRS and SEM.

In the first chapter an introduction about CNTs, CF, ATR polymerization, PCM and work description is given. The second chapter is totally concerned with MWNTs work which contains detailed information of MWNTs and living polymerization, materials and equipments, experimental procedures and characterization and discussions related to this study.

In the third chapter the detailed introduction to CF and its surface modification, polymer matrix, experimental procedures and characterization & discussions related to this study were given.

In the fourth chapter the results and conclusions on both the works are described. The work concludes by giving some suggestions for future works.

Contents

List of Figures

List of Tables & Equations

Equations

List of Abbreviations

ATRP……..Atom Transfer Radical Polymerization
$CDCl_3$……..Deuterated Chloroform
CF……Carbon fibers
$CHCl_3$……..Chloroform
C, H and N……..Carbon, Nitrogen and Hydrogen
Cm……..Centimeter
CNT……..Carbon nanotubes
Cu(I)Br……..Copper (I) bromide
CVD……...Chemical Vapor Deposition
℃……Degree Celsius
DMF……Dimethylformamide
DMAP……Dimethylaminopyridine
DWNTs……...Double-walled Carbon nanotubes
EA……...Elemental analysis
FTIR……Fourier Transform Infrared Spectroscopy
GPa……Gigapascal
g……..Gram
HiPCO……High-Pressure CO Conversion
^{1}H NMR……Proton Nuclear Magnetic Resonance
HNO_3……..Nitric acid
I_G/I_D……..Intensity ratio of D band and G band
K……..Kelvin (absolute temperature scale)
KBr……Potassium bromide
LRS……Laser Raman spectroscopy
m.....Meter
min……..Minute
mL……...Milliliter
mm……....Millimeter
mmol……...Millimole
MPa……Megapascal
MWNTs……..Multi-walled Carbon nanotubes
MWNT-COOH…….. Oxidized Multi-walled Carbon nanotubes
MWNT-OH……Diol functionalized Multi-walled Carbon nanotubes
N……..Normal (unit of concentration)
NaOH……..Sodium hydroxide
nm…….. Nanometer
PAN……Polyacrylonitrile
PCM……...Polymer Composite Materials
PMDETA……Pentamethyldiethylenetriamine
PtBA……Poly *tert*-Butyl Acrylate
RAFT…….. Reversible Addition-Fragmentation Chain Transfer
RFGF……Raman Frequency Gauge Factor or Shift Factor
rpm……Revolutions per minute
S……..Second (base unit of time)
SEM……Scanning Electron Microscopy
$SOCl_2$……....Thionyl Chloride
t-BA……..*tert*-Butyl Acrylate
TEM……Transmission Electron Microscopy
TGA……Thermo Gravimetric analysis
THF……Tetrahydrofuran
TPa……..Terapascal
W……....Watt
Wt……..Weight
µL……Microliter
υ_o ……Frequency of the incident light

CHAPTER I – INTRODUCTION

1. BRIEF INTRODUCTON ON MWNTs, CF, ATRP & PCM

Newer technologies demand new materials. Polymer composite materials (PCM), with their wide range of possible reinforcements and polymers, open the way to an enormous class of materials with differing chemical, physical, and mechanical properties. Therefore the ultimate goal of today's polymer composite research is to formulate procedures in an attractive way that leads to design composites with specified and enhanced properties that can meet a broad range of applications. The reinforcements in PCM can be from a wide range of materials such as metals, semiconductors, organic and inorganic particles, fibers, carbon structures (e.g. CNT, CNF and CF) and ceramics with their size ranging from nanometer to millimeters. As one of the most interesting reinforcing materials, carbon based structures (CNT, CNF and CF) have received significant attention in terms of fundamental properties and potential applications.

Nanotechnology offers new design, characterization, production, and application of systems, devices and materials at the nanometer scale. Carbon nanotubes are promising nanotechnology building blocks. Carbon nanotubes (CNT) are an exciting allotrope of carbon that were discovered a decade ago by Iijima [1] and are generally considered to belong to the fullerene family. Since their discovery, carbon nanotubes have attracted the attention of many scientists around the world. This extraordinary interest stems from their outstanding structural, mechanical, thermal and electrical properties. For example, the measured specific tensile strength of a single layer of a multi-walled carbon nanotube can be as high as 100 times that of steel, and the graphene sheet (in-plane) is as stiff as diamond at low strain [2].

Their application potential in many fields of science was anticipated from the very beginning and the number of researchers that are studying and implementing them are increasing every day. Carbon nanotubes show strong application potential in reinforced composite materials, electronics, components of nanoelectronic technology [3], as probes in scanning probe microscopy [4], in high-sensitivity microbalances [5], in hydrogen storage devices [6], in field emission type displays [7], as electrodes in organic light-emitting diodes [8], as tiny tweezers for nanoscale manipulation [9], as gas detectors [10], chemical and biological sensing, and in many more areas. While some of the proposed applications remain still a far-off dream, others are close to technical realization.

CF is the other carbon structure which is also extensively used as reinforcement in polymer composite materials. Carbon has different physical forms which are diamond, graphite and amorphous, and carbon fibers can be produced in both crystalline and amorphous form.

Carbon fibers which are produced in crystalline form have high modulus and can be considered for reinforcement purposes [10a]. The first carbon fibers were produced for the use as filaments in the first incandescent lamps by pyrolysis of linen or bamboo fiber [10b]. High performance carbon fibers were first produced in the early 1960s in England [10c]. Fiber reinforced polymers offer a mixture of strength and modulus, which are comparable to or even better than, many traditional metallic materials. Some of these properties such as the specific gravity, strength-weight ratio and modulus-weight ratio are superior to those of metallic materials [10d].

Nowadays, polymers play a very important role in numerous fields of everyday life due to their advantages over conventional materials (e.g. wood, clay, metals) such as lightness, resistance to corrosion, ease of processing, and low cost production. Besides, polymers are easy to handle and have many degrees of freedom for controlling their properties. Further improvement of their performance, including composite fabrication still remains under intensive investigation. The altering and enhancement of the polymer's properties can occur through doping with various nanofillers such as carbon structures, metals, semiconductors, organic and inorganic particles and fibers, as well as and ceramics [11-14]. Such additives are used in polymers for a variety of reasons, for example: improved processing, density control, optical effects, thermal conductivity, control of the thermal expansion, electrical properties that enable charge dissipation or electromagnetic interference shielding, magnetic properties, flame resistance, and improved mechanical properties, such as hardness, elasticity, and tear resistance [15-17].

Many experiments indicate that carbon nanotubes/polymer composites are weaker or only slightly stronger than the neat polymer [18]. This has been found to be primarily due to a combination of several factors, namely

(1) Poor dispersion of nanotubes
(2) Inadequate alignment of nanotubes
(3) Weak interfacial bonding between the carbon nanotubes and polymer matrix

Hence the manufacture of CNTs reinforced composites mainly depends on the following factors [19] –

(1) Homogeneous dispersion of the CNTs in the polymer matrix
(2) Strong interfacial adhesion between the carbon nanotubes and the matrix to enable stress transfer from the matrix to the reinforcing element

So the use of carbon nanotubes as reinforcing components in polymer composites requires tailoring the nature of nanotubes walls in order to control the interfacial interactions between the nanotubes and polymer chains. These interactions govern the load-transfer efficiency from the polymer to the nanotubes and hence the reinforcement efficiency. One of the ways to tailor the surface of carbon nanotubes is by chemical functionalisation that introduces functional groups which promote covalent or van der Waals forces between the matrix and the nanofillers [20]. The effect of a linkage between the nanotubes and the polymer, which should lead to improved interfacial interactions, is confirmed by calculations by Frankland et al. [21] from which it is predicted that a functionalisation of less than 1% would improve the interaction between nanotubes and the polymer without decreasing their strength significantly.

In the case of Carbon fibers, Carbon fibers have poor wettability and adsorption by most polymers is difficult because carbon fiber surface is a non-polar compound of highly crystallized graphitic basal planes with inert structures. As a result, the interfacial bonding strength between the fibers and polymer matrices is low, and good mechanical performance of composites can not be ensured [22-24]. Mechanical properties of the composite are highly dependent on interface between the CF and the polymer matrix. If the interface is weak, the load carrying capabilities of the composite will be reduced drastically. The interaction of a fiber with a matrix material depends strongly on the chemical/molecular features and atomic composition of the fiber surface layers as well as its topographical nature [25]. In order to improve the wettability of carbon fibers and interfacial adhesion of composites, several techniques for surface treatment on carbon fibers have been applied, including plasma [26, 27], electrochemical oxidation [28-29], wet chemical [30-31] and thermal treatment [32-34]. These treatments on carbon fibers improved interfacial wetting and adhesion force of the final composites to some extent, but they had the drawbacks of high cost, high energy consumption and significant loss in single fiber strength.

New novel polymerization mechanisms such as ATRP allows the preparation of a wide range of different materials which are either difficult to prepare, or not available via other polymerization processes. For example, the architecture or topology of the polymer (i.e. comb, star, dendrite, etc.), composition of the backbone (i.e. random, gradient, or block copolymer), inclusion of functionality (i.e. chain end, site specific, etc.) can all be readily manipulated using living free radical methodologies while still retaining a high degree of control over the molecular weight and polydispersity. Controlled or living polymerization technique can promote the growth of oligomers from a specific modified surface in a controlled manner. Based on the above advantages, amongst the methodologies available for the preparation of MWNTs based hybrid nanomaterials, controlled or living polymerization technique would be optimal [35]. One of the most successful process is atom transfer radical polymerization (ATRP). ATRP reactions are

used effectively to modify the surfaces of a few nanostructured carbon materials, such as carbon nanotubes and carbon black [36]. The radical reactions involved in the ATRP process enables to use wide range of monomers leading to polymer-modified surfaces with new functionality and the covalent bonding between the carbon surface and polymers can highly increase the interaction affinity nanotube-matrix during processing.

2. WORK DESCRIPTION

The overall project consists of two approaches

Part-1. Studies on polymer/carbon based nanoparticles (MWNT-based nanocomposites)- Surface modification and polymerization process.

Part-2. Applying the surface modification for tailoring the surface of CF and studies on the interfacial properties of surface modified carbon fiber/ epoxy reinforced composites.

The main objective of the work "studies on polymer/ carbon based nanoparticles (MWNT-based nanocomposites)" comprises of the following main steps

- Oxidation of MWNTs with nitric acid
- Characterization of modified MWNTs.
- Diol spacer Functionalisation and Characterization
- Anchoring initiator to modified Carbon nanotubes
- Polymerisation (ATRP) of polymer chains from the modified carbon nanotubes surface

The surface modification of the MWNTs and polymerization reactions were initially investigated at the University of Aveiro (UA, Portugal), searching for a correct process & process conditions. Later, this surface modification process was applied on CF and further studies were done. This aspect is crucial in the preparation of composites, as the interaction reinforcement (either MWNTs or CF) /polymer is necessarily determined by the chemical nature of the reinforcing surface.

The detailed procedures are described below.

Surface oxidation - Various methods of functionalization of MWNTs were available in order to achieve a good level of exfoliation of the bundles and agglomerations of MWNTs. Covalent functionalization represents an efficient way to render the MWNTs soluble either in aqueous or organic phase, by attaching different functional groups directly to the MWNTs [37]. Literature screening shows that nitric acid is extensively used to oxidize MWNTs [73, 73a, 74]. Nitric acid treatment produces mainly carboxylic groups [38–40] which contribute to the solubilization of the nanotubes [41, 42]. In the present study the oxidation of MWNTs with nitric acid was investigated.

Anchoring of diol spacer - In order to promote an even better MWNTs-matrix interaction, the acid oxidized nanotubes were submitted to a subsequent treatment where a diol spacer (MWNTs-OH) attached to nanotube surface. This procedure also allows the production of macro initiators for the atom transfer radical polymerization (ATRP) of *tert*-butyl acrylate (*t*-BA) [43].

Mechanism of polymerization - Atom transfer radical polymerization (ATRP) mechanism was used in order to grow polymer chains from the carbon surface.

Characterization of Modified Nanotubes - Each modified material was submitted to Fourier transformed infrared analysis (FTIR), Thermo gravimetric analysis (TGA), Scanning electron microscopy (SEM), Transmission electron microscopy (TEM), Solubility test and Elemental analysis. Polymerized MWNTs are also subjected to liquid state ^{1}HNMR spectroscopy (Proton NMR).

Spectroscopic methods (FTIR and ^{1}HNMR) were used for identifying the presence of functional groups or polymers on the nanotube surface.

The TGA was used to evaluate the thermal and thermo-oxidative stability of the nanotubes. These measurements provide information about the nanotubes chemical structure. Furthermore, they enable the determination of the start temperature degradation (STD) and characteristics of the produced polymers degradation process under nitrogen and synthetic air.

SEM was employed in order to study the morphology of the MWNTs. The possible degradation and diameters of nanotubes were also assessed.

TEM analyses were conducted in order to have images with higher magnification than SEM. Surface of tubes could be more deeply investigated.

Solubility tests in water and organic solvents were made in order to have an idea of the polarity of the neat and treated MWNTs.

Elemental analysis was done to determine the atomic percentage of the elements in the samples.

With the acquired theoretical and experimental knowledge and from the attractive results on the surface modification process of carbon nanotubes my work further stepped towards the surface modification carbon fibers. The same surface modification process used for MWNTs was applied for modifying the surface characteristics of CF and thereby to facilitate

enhanced adhesion between the CF and a matrix material. Surface modification of CF was done in University of Aveiro (UA, Portugal) and further work with the modified CF producing composite and its analysis was carried out in Aalborg University (AAL, Denmark).

The second part of the work consists of the following steps

1. Surface modification of carbon fibers
    1. Surface treatment CF using nitric acid
    2. Followed by diol spacer functionalization
    3. Modified CF surface characterization using SEM and LRS

2. Manufacturing of short single fiber composite specimens (using surface modified CF)

3. Examination of carbon fiber/ matrix interface through tensile test insitu Laser Raman spectroscopy - Determination of interfacial strength of functionalized CF epoxy composite

CHAPTER II- CARBON NANOTUBES

1. CARBON NANOTUBES

1.1 STRUCTURE AND PROPERTIES

Carbon nanotubes (CNT) were discovered in 1976 when Endo [84] synthesized vapor-grown carbon fibers, however at the time, it was not given any thought and focus. It was only after Iijima's work in 1991 [1] that global scientific attention was turned to these interesting carbon structures and intense studies on the properties, structure and applications of these unique materials have been carried out.

CNTs are considered to be a rolled-up graphene sheet that forms long concentric cylinders. Bonding in CNT is essentially sp^2, the circular curvature causes σ bonds to be slightly out of plane, whilst the π orbital is more delocalized outside the tube [44]. The properties of nanotubes depend on the structure, morphology, diameter, and length of the tubes. The structure of carbon nanotubes is described in terms of the tube chirality, which is defined by the chiral vector C_h and the chiral angle θ (Figure 1). The chiral vector indicates the way, in which graphene is rolled-up to form a nanotube. The chiral vector is described as [45]:

$$\vec{C}_h = n\vec{a}_1 + m\vec{a}_2 \qquad \text{Equation-1}$$

Where the integers (*n, m*) indicate the number of steps along the zigzag carbon bonds of the hexagonal lattice, $a_1$and a_2 are unit vectors (figure 1). If m=0, the nanotubes are called "zigzag". If n=m, the nanotubes are called "armchair". Otherwise, they are called "chiral". The chirality of the carbon nanotubes has a huge impact on their properties, especially electronic ones.

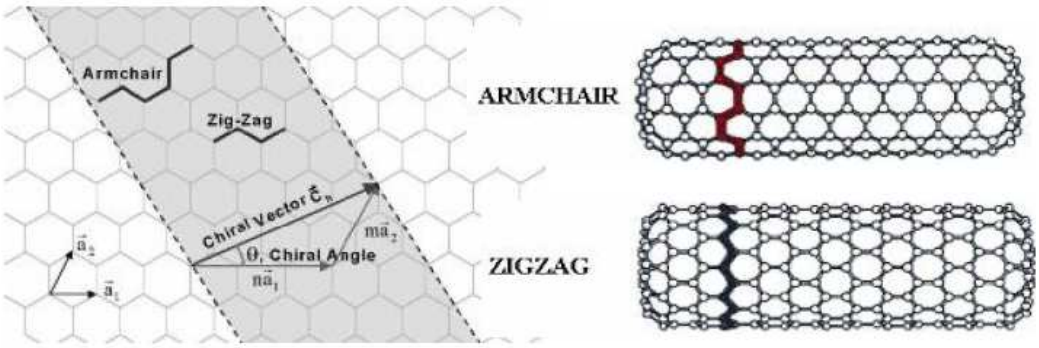

Figure-1: Chiral vector of SWCNT, chiral directions into the carbon sheet and examples of SWCNT: armchair (right top), zigzag (right bottom) [122]

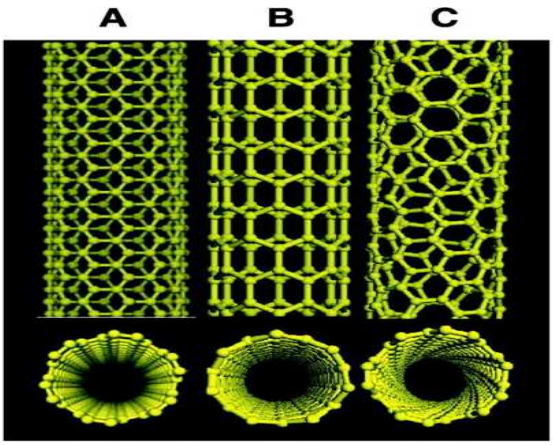

Figure-2: Different SWNTs [123]
A. armchair SWCNT
B. zigzag SWCNT
C. chiral SWCNT

PROPERTIES OF CNT´s

Carbon nanotubes have gained in interest as nanoscale materials due to their exceptional, outstanding properties such as: extremely high Young's modulus and ultimate strength, high electric and thermal conductivity. More details on the properties of carbon nanotubes are presented below.

Mechanical properties

The structural properties of CNTs with strong σ bonds between the carbon atoms give nanotubes a very high Young's modulus and tensile strength. The strength of the carbon-carbon bonds in-plane, along the cylinder axis makes the structure exceptionally strong resistance to any failure. CNTs also have very good elasto-mechanical properties. The two dimensional (2D) arrangement of the carbon atoms in a graphene sheet permits a large out of- plane distortion. Both experimental and theoretical investigations show extraordinary mechanical properties of individual MWNTs with Young's modulus being over 1 TPa and a tensile strength of 10 - 200 GPa [133-135], which is several hundred times more than that of steel, while they are only one-sixth as heavy. The elastic response of a nanotube to deformation is also remarkable: CNTs can sustain up to 15 % tensile strain before fracture. Nanotubes are shown to be very flexible, with the reversible bending up to angles of 110º for both SWNT and MWNT [136]. Due to the extremely high strength of CNTs, they can bend without breaking. All of these properties open up broad possibilities for the use of CNTs as lightweight, highly elastic, and very strong composite fillers [47].

Material	***Young Modulus (TPa)***	***Tensile Strength (GPa)***
SWNT	~1 (from 1 to 5)	13-53[E]
MWNT	0.8-0.9	150
Stainless Steel	~0.2	~0.65-1
Kevlar	~0.15	~3.5

Table -1: Comparison of mechanical properties of different materials [137]

The mechanical properties of other reinforcing materials are compared with CNTs in table-1(a) to place the mechanical properties of CNTs in to proper perspective.

Fiber	Diameter (μm)	Density (g/cm^3)	Tensile strength (GPa)	Young's Modulus (GPa)
Carbon	7	1.66	2.4~3.1	120~170
Glass	14	2.5	3.4~4.6	90
Aramid	12	1.44	2.8	70~170
Boron	100-140	2.5	3.5	400
Quartz	9	2.2	3.4	70
SiC	10-20	2.3	2.8	190
CNTs	0.001~0.1	1.33	50~200	~1000

Table-1(a): Comparison of mechanical properties of different reinforcing materials [138]

Conventional fibres when subjected to stress beyond the elastic limit are susceptible to fracture. One of the properties which make nanotubes different from conventional carbon fibres and all other currently known fibres is, that they can return to their original straight form when the applied stress on the nanotube is released. This raises the fascinating possibility that composites could be produced which would snap back into place following deformation.

Chemical properties

Due to the curvature effect of the surface, CNTs have enhanced chemical reactivity compared with a graphene sheet. High curvature of Carbon nanotube end caps is the driving force for its reactivity. For the same reason, a smaller nanotube diameter results in increased reactivity. Functionalization of the carbon nanotubes (chemical or physical modification of the surface of CNTs, e.g. by the attachment of certain molecules or functional groups) is a very important issue in order to overcome their poor solubility in solvents. Functionalized CNTs are

very significant for chemical and biological applications because of their strong sensitivity to chemical or environmental interactions. This leads to a broad range of applications, e.g. as sensors. Covalent and non-covalent functionalization, doping, decoration with organic as well as inorganic species of the surface of CNTs lead to direct changes of the properties of carbon nanotubes (optical, electrical, and mechanical) [141].

Electrical Properties

Carbon nanotubes possess unique electrical properties. Because of the symmetry and unique electronic structure of graphene, the structure of a nanotube strongly affects its electrical properties. The differences in the conducting properties of CNTs are caused by their molecular structure. CNTs can either be conducting or semiconducting, depending on their chirality [139]. Nanotubes are metallic, if the integers of equation -1 are: $n=m$ (armchair structure) and $n-m=3i$ (where i is an integer). All other structures are predicted to be semiconducting that is, nanotubes (5,0), (6,4), (9,1), etc. are semiconducting [140].

Thermal properties

All nanotubes are expected to be very good thermal conductors along the tube, exhibiting a property known as "ballistic conduction", but good insulators laterally to the tube axis. It is predicted that carbon nanotubes will be able to transmit up to 6000 watts per meter per kelvin at room temperature whereas copper, a metal well-known for its good thermal conductivity only transmits 385 W/(m.K). The temperature stability of carbon nanotubes is estimated to be up to 2800 degrees Celsius in vacuum and about 750 degrees Celsius in air [126].

1.2. TYPES OF CNTs

Nanotubes are mainly categorized as single-walled nanotubes (SWNTs) and multi-walled nanotubes (MWNTs).

Single-walled nanotubes (SWNTs)

A single-walled carbon nanotube (SWNT) is a one-atom thick sheet of graphite (called graphene) rolled up into a seamless cylinder with diameter in the order of a nanometer. This results in a nanostructure where the length-to-diameter ratio exceeds 1,000,000 and which are defined by their diameter and their chirality [44, 46]. Depending on the chirality SWNTs may either be metallic or semiconducting.

Multiwalled carbon nanotubes (MWNTs)

Multiwalled carbon nanotubes (MWNTs) are a group of concentric SWNTs (shown in figure 3) often capped at both ends, with diameters in the range from several nanometers up to 200 nm [44, 45]. These concentric nanotubes are held together by van der Waals bonding. MWNTs form complex systems with different wall numbers, structures, and properties and additional features such as: tips, internal closures within the central part of the tube, forming a so called “bamboo” structure (Figure 3), and even an angle Y-junction formation of MWNTs.

There are two models which can be used to describe the structures of multi-walled nanotubes. In the Russian Doll model, sheets of graphite are arranged in concentric cylinders, e.g. a single-walled nanotube (SWNT) within a larger single-walled nanotube. In the Parchment model, a single sheet of graphite is rolled in around itself, resembling a scroll of parchment or a rolled up newspaper. The interlayer distance in multi-walled nanotubes is close to the distance between graphene layers in graphite, approximately 3.3 Å (330 pm).

Double Walled Carbon nanotubes

The special types of CNTs are double-walled carbon nanotubes (DWNTs) (figure-4). The double-walled nanotubes have a coaxial structure, containing two concentric graphene cylinders. They contain very similar morphology and properties as compared to SWNT, while improving significantly their resistance to chemicals. This is especially important when functionalization is required to add new properties to the CNT. In the case of SWNTs, covalent functionalization will break some C=C double bonds, leaving "holes" in the structure on the nanotube and thus modifying both its mechanical and electrical properties. Double-walled carbon nanotubes have higher thermal and chemical stability than single-walled carbon nanotubes, and can be applied to gas sensors, dielectric devices, nanoelectronic devices, nanocomposites and emitters etc.

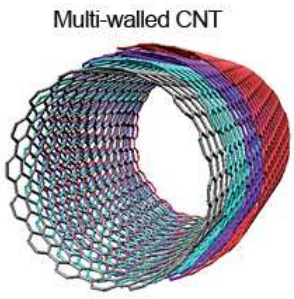

Figure-3: Multiwalled CNTs [124]

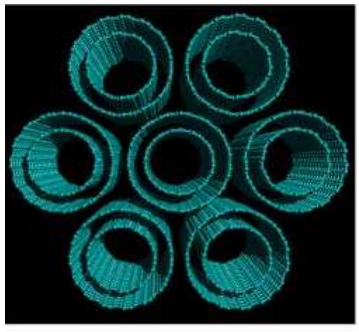

Figure-4: Double-walled CNTs [125]

1.3. MANUFACTURING METHODS

At present carbon nanotubes are manufactured by different methods in laboratories and industries. There are numerous variations in these techniques operating under different conditions, with different set-ups, and process parameters. Every technique provides diverse advantages and disadvantages over the quality and kinds of synthesized CNTs. An overview of these techniques is given in table 2. Nowadays, the production of CNTs with a higher yield, large-scale, low costs, and uniformity are still the biggest issues in the carbon nanotube society.

Table 2: An overview on the most common CNTs synthesis techniques and their advantages and disadvantages [126].

Method	***CVD***	***Arc Discharge***	***Laser Ablation***	***HiPCO***
Basics	Decomposition of hydrocarbon gases in the presence of metal catalyst particles	Electric arc discharge generated between two graphite electrodes under an inert atmosphere (argon, helium)	Graphite target is vaporized by laser irradiation under flowing inert atmosphere and high temperature	Gas-phase growth of SWNT with carbon monoxide at high temperature and pressure
SWNT	long, 0.6- 4 nm diameter	short, 1.2-1.4 nm diameter	long, 1-2 nm diameter	~0.7 nm diameter, various lengths
MWNT	long, 10-200 nm diameter	short, 1-3 nm diameter	not applicable but possible	not applicable
Yield	up to 100%	up to 90%	up to 65%	up to 70%
Advantages	high purity, large scale production, simple	easy, defect-free nanotubes, no catalyst	high purity, defect free SWNTs	large scale, high purity
Disadvantages	limited control over the structures, defects	short, tangled nanotubes, random structures	expensive, low scale production	defects

1.4. CHEMICAL MODIFICATION

CNTs in all their forms are difficult to disperse and dissolve in any organic and aqueous medium. Due to the strong attractive long-ranged van der Waals interactions, nanotubes tend to aggregate and form bundles or ropes, usually with highly entangled network structures. Homogenous dispersion of CNTs within a supporting medium is crucial for the fabrication of composites with improved properties, well defined and uniform structures. This issue stimulates intensive studies on the exfoliation of carbon nanotubes. There are commonly two ways to functionalize the CNTs: the covalent attachment ("grafting-to" and "grafting-from") [50-52] of chemical groups and the non covalent adsorption or wrapping. (Polymer wrapping [53, 54], π-π stacking interaction [55], adsorption of surfactants [56]).

Covalent functionalization:

Covalent methods refer to a treatment that involves bond breaking across the surface of the CNTs (e.g. by oxidation) which disrupts the delocalized π-electron systems and fracture of σ-bonds. Hence, leads to incorporation of other species across the CNTs surface. Introducing defects to the CNTs shell significantly alters the optical, mechanical and electrical properties of the nanotubes and leads to an inferior performance of the composites [57]. There are many strategies to functionalize CNTs with organic or inorganic moieties through chemical bonding. For example, CNTs can be chemically anchored at the end, defect, and side-site by metal complexes, organic moieties, solution-phase ozonolysis. In addition, oxidation and electrochemical modification have been used to modify the CNTs surfaces [58].The advantage is that this kind of modification may improve the efficiency of the bonding between nanotubes and the host material. Therefore, the interfacial stress transfer between the matrix and CNTs may be enhanced leading to better mechanical performance.

Non-covalent functionalization:

Many polymer molecules and surfactants can be applied to interact with nanotubes surfaces via physical bonding between them. The interaction is based on van der Waals or π- π bonding. This modification of the carbon nanotubes is of great advantage because no disruption of the sp^2 graphene structure occurs i.e. no effect on the electronic structure of carbon nanotubes and the CNT properties are preserved. Its disadvantage concerns weak forces between wrapped/coupled molecules (low bonding strength) that may lower the load transfer in the composite [59].

1.5. CNT OXIDATION

Despite the outstanding properties like high Young's modulus and low density of CNTs their insolubility hinders the transfer of those properties into the bulk. Though they are very interesting fillers for reinforcement of polymer composites, lack of surface functional groups results in inadequate adhesion in composite materials with polymeric matrices. Covalent functionalization represents an efficient way to render the CNTs soluble either in aqueous or organic phase, by attaching different functional groups directly to the CNTs [60]. Chemical modification and covalent functionalization of CNTs with several organic species like alcohols, amines and polymers can be done in many ways as reported elsewhere [61-64]. Literature screening shows that nitric acid is extensively used to oxidize CNTs [73, 73a, 74].

The generation and functionalization of defect sites at the end or side walls of the nanotubes by oxidation is a well known exohedral functionalization technique [65]. Carbon nanotubes upon the treatment under oxidative conditions, the defect sites on the surface of CNT are transferred to carboxylic acid moieties. Nitric acid treatment (oxidative conditions) produces mainly carboxylic groups [66–68, 73, 73a, 74] and the presence of (modified) carboxyl groups leads to a reduction of van der Waals interactions between the CNTs, which strongly facilitates the separation of nanotube bundles into individual tubes. These –COOH groups not only contribute to the solubilization of the nanotubes [69, 70] but also allows covalent linkages of oligomers or polymers with the nanotubes [71, 72].

Iosif Daniel Rosca [73], Qiao Chen [73a] and Chao Gao [74] studied the oxidation of MWNTs with nitric acid at different conditions. Nanotubes functionalized by refluxing in nitric acid under less vigorous conditions basically retain their pristine electronic and mechanical properties [75] and also minimizes the shortening of the tubes.

The surface area and the oxygen amount on the surface increase with the oxidation time. The reaction conditions differ largely from one author to another, e.g., the acid concentration varies in the range of 15–70 wt%, the initial concentration of the CNTs varies from 0.1 to 10 mg/mL, and the treatment duration from 1 to 48 h. The oxygen was present as the following functional groups: esters, anhydrides, phenols, ethers and carboxylic acids. They also worked on the characterization techniques like FTIR, ^{1}H NMR, ^{13}C NMR, SEM, and TEM. They also used TGA to detect the presence of functional groups on the MWNTS surface and studies were also carried out in order to measure the degradation temperature of each functional group under inert atmosphere.

2. LIVING POLYMERIZATION

In polymer chemistry, living polymerization is a form of addition polymerization where the ability of a growing polymer chain to terminate has been removed [76]. This can be accomplished in a variety of ways. Chain termination and chain transfer reactions are absent and the rate of chain initiation is also much larger than the rate of chain propagation. The result is that the polymer chains grow at a more constant rate than seen in traditional chain polymerization and their lengths remain very similar (i.e. they have a very low polydispersity index).

Living polymerization is a popular method for synthesizing block copolymers since the polymer can be synthesized in stages, each stage containing a different monomer. Additional advantages are predetermined molar mass and control over end-groups. Living polymerization in the literature is often called "living" polymerization or controlled polymerization. Living polymerization was demonstrated by M. Szwarc in 1956 in the anionic polymerization of styrene with an alkali metal / naphthalene system in THF. He found that after addition of monomer to the initiator system that the increase in viscosity would eventually cease but that after addition of a new amount of monomer after some time the viscosity would start to increase again [77].

Very late in the twentieth century several new methods were discovered which allowed the development of living polymerization using free radical chemistry. These techniques involved catalytic chain transfer agent, metastable free radical mediated polymerization, reversible addition-fragmentation chain transfer (RAFT) polymerization and atom transfer radical polymerization (ATRP). The last technique is described below and is used in this work in order to grow polymers from the Multi walled carbon nonotubes [78].

2.1. ATOM TRANSFER RADICAL POLYMERIZATION

Covalent attachment of polymer chains to the surface can be accomplished by either “grafting to” or “grafting from” techniques. “Grafting to” involves the bonding of a preformed end-functionalized polymer to reactive surface groups on the substrate. The “grafting from” technique involves the immobilization of initiators onto the substrate followed by in situ surface polymerization to generate the tethered polymer chains [79, 80]. It has the advantage of preparing polymer brushes with high grafting density (up to 85 mg/m^2) as compared to the “grafting to” method (about 1 mg/m^2) [81]. Indeed, the attachment of a small number of chains hinders diffusion of additional macromolecules to the surface, thereby leading to low grafting density. A high polymer chain density is actually of considerable importance when dealing with polymer-based biocompatible materials.

For better control of the molecular weight and the molecular weight distribution of the polymer chains, living radical, anionic, cationic, and ring-opening metathesis polymerizations have been used in “grafting from” methods [79]. Controlled radical polymerization, especially atom transfer radical polymerization (ATRP) [82] is the most used method to graft polymer chains of controlled molecular weight from, e.g. silicon wafers, gold particles, and polymer backbones. ATRP is indeed a versatile method in terms of choice of functional monomers, performance at moderate temperature (100 ˚C or less), in either aqueous or organic solvents [83]. A variety of polymeric materials can be obtained by ATRP ranging from simple linear macromolecules to more sophisticated architectures such as star brush copolymers [83].

Atom transfer radical polymerization or ATRP involves the chain initiation of free radical polymerization by a halogenated organic species in the presence of a metal halide species. The metal has a number of different oxidation states that allows it to abstract a halide from the organohalide, creating a radical that then starts free radical polymerization. After initiation and propagation, the radical on the active chain terminus is reversibly terminated (with the halide) by reacting with the catalyst in its higher oxidation state. Thus, the redox process gives rise to equilibrium between dormant (Polymer-Halide) and active (Polymer-Radical) chains. The equilibrium is designed to heavily favor the dormant state, which effectively reduces the radical concentration to sufficiently low levels to limit bimolecular coupling. Obstacles associated with this type of reaction are generally low solubility of the metal halide species, which results in limited availability of the catalyst. This is improved by the addition of a ligand, which significantly improves the solubility of the metal halide and thus the availability of the catalyst but complicates subsequent catalyst removal from the polymer product [78].

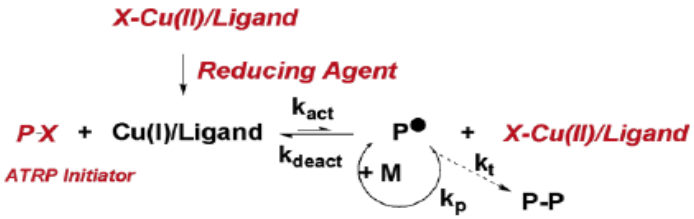

Figure 5: ATRP schematic representation [59].

3. MATERIALS AND EQUIPMENTS

3.1. MWNTs

The MWNTs used in the present work were supplied by Shenzhen Nanotechnologies Co. Ltd (NTP). It is a High-Tech company focusing on the R&D, manufacture and application of carbon nanotubes and ranked as one of the top manufacturers and as a leader in the global carbon nanotube industry.

Purity	>95%
Diameter	60-100 nm
Length	5-15 μm
Amorphous carbon	<3%
Ash (catalyst residue)	<0.2 wt%
Special surface area	40-300 m^2/g
Thermal conductivity	~2800 W/m-K
Interlayer Distance	0.34 nm
Pore Volume	0.8 cm^3/g
Electric conductivity	10E-4 s/cm
Ablating Temperature	>550 ºC (in air) 3500 ºC(in inert atmosphere or vacuum)
I_G/I_D (Raman data)	$0< I_G/I_D <2$

Table-3: Properties of MWNTs used in the present work [127].

3.2. REAGENTS

Tert-butyl acrylate (99%) was purchased from Sigma- Aldrich and purified by alumina powder. HNO_3 (65%), N,N,N,N PMDETA (99%), N,N,-Dimethylformamide (99.8%), Cu(I) Br (99.99%), 2-Bromo-2-methylpropionyl bromide (99.99%). $SOCl_2$ (99). Acetone (99.5%), Chloroform (98%) and Methanol (99.8%) were purchased from Panreac. THF (99.5%) was purchased from Carlo Erba. Toluene (99.7%) and Triethylamine (99%) were purchased from Riedel-de Haen. Ethylene Glycol was purchased from Sigma chemicals.

3.3. MEASUREMENT ANALYSES

Fourier Transform Infrared Spectroscopy (FTIR)

Fourier transform infrared spectra were recorded on a Matson 700 FTIR spectrometer using dry KBr disks.

Electron Microscopy

Scanning Electron Microscopy (SEM) images were obtained using a FEG-SEM Hitachi S4100 field emission microscope. Transmission Electron Microscopy (TEM) images were obtained using a Hitachi H-9000 Electron Microscope.

Thermo gravimetric analysis

The TGA measurements were carried out in a TGA50 SHIMADZU, with the heating rate 10 ℃/min under the nitrogen flow (20 mL/min) and s ynthetic air (20 mL/min) flow .These measurements were done under Nitrogen and synthetic air atmospheres with starting and ending temperatures 25 ºC & 950 ºC.

NMR Spectroscopy

Proton NMR Broker Avance/300 with frequency 300 MHz and solvent $CDCl_3$ were used.

Elemental analysis

Elemental analysis is a process where a sample is analyzed for its elemental and sometimes isotopic composition. Elemental analysis can be qualitative determining what elements are present, and it can be quantitative determining how much of each are present. Elemental analysis or "EA" almost always refers to CHNX analysis, determination of the percentage weights of carbon, hydrogen, nitrogen, and heteroatoms (X) (halogens, sulphur) of a sample. This information is important to help determine the structure of an unknown compound, as well as to help prove the structure and purity of a synthesized compound [78]. The samples pristine MWNT, MWNT-COOH, MWNT-OH are dried well and then subjected to analysis in an Elemental Analyser Leco CHNS-932 for the determination of percentages of C, H and N atoms.

3.4. Solubility Tests

Solubility tests in water and organic solvent were carried out in order to assess the polarity of the functionalized MWNTs. A small amount (same amount of each sample is used) of tubes was dispersed in vials with the same amount of solvent. The mixtures were sonicated for 5 min and allowed to rest for 30 min prior to investigation.

4. EXPERIMENTAL PROCEDURE

4.1. OXIDATION OF MWNTs WITH HNO_3(MWNT-COOH)

Batch -1

200mg of MWNTs were taken in a two necked round bottom flask containing a magnetic stirrer and equipped with reflux condenser and nitrogen inlet. About 7 mL of nitric acid (65%) is added to this round bottom flask containing MWNTs and the mixture is sonicated for 35 minutes at 40 ºC.

After sonification, ensuring that the MWNTs are well dispersed (without any agglomerates), the mixture is heated (oxidized) in oil bath using heating pan (equipped with magnetic stirring) at 80 ºC for 4 hours with continuous stirring under nitrogen atmosphere. Oxidation is carried out under nitrogen atmosphere as nitrogen acts as antioxidant gas and prevents oxidation of MWNTs by atmospheric oxygen ensuring the oxidation is carried out, only by nitric acid.

After this, the remainents which are in acidic medium are neutralized by washing with distilled water and a small amount of 0.1 N NaOH. The oxidized MWNTs in the solution (neutralized) was divided into 2 polyethylene tubes, with the same mass in each one, and centrifuged at 15000 rpm for 45 min at 5 ºC. Most of the MWNTs were deposited at the bottom of the flask, so the excess solution was removed through decantation, with the help of a Pasteur pipette. The resultant oxidized MWNTs are rinsed and filtered and then rinsed several times with distilled water to remove the neutralization products and decanted.

The oxidized MWNTs (MWNT-COOH) are then subjected to filtration using sintered filter under vacuum. The solid MWNTs are then subjected to drying at 105 ºC for 48 hours (till constant weight is attained).

The dried MWNT-COOH was characterized using TGA, FTIR, SEM, TEM, solubility test and elemental analysis.

Note - After the first batch the following changes are done in the second and preceding batches

1. Sonication is done under nitrogen atmosphere.
2. MWNTs agglomerates are mechanically pressed to get powdered MWNTs for complete surface exposure to reaction.
3. Centrifugation step is removed.

Batch -2

The same procedure and reaction conditions are applied for the next batches with the above changes applied and without centrifugation step and sonication for 15 min.

Batch No.	Wt. of MWNTs (Grams)	Nitric acid used (mL)	Sonicaion time (minutes) & Oxidation time(Hours)
2	0.5702	17.5	15 & 4
3	1.0328	30	20 & 4
4	1.0844	30	20 & 4
5	1.1632	40	20 & 4

Table- 4: Amount of MWNTs, acid and process conditions used in each batch.

4.2. FUNCTIONALISATION OF MWNT-COOH WITH DOIL SPACER (MWNT-OH)

Preparation of MWNT-COCl (Batch-6)

Into a 100 mL two neck round-shaped flask equipped with a condenser, an amount of 256.7 mg of MWNTs-COOH was suspended in 15 mL of $SOCl_2$ (thionyl chloride).The suspension was stirred at 65 ℃ for 24 hours. After 24 hours the remaining liquid was removed or evaporated under nitrogen flux at 40 ℃ leaving solid MWNTs-COCl in the flask for further reaction.

Preparation of MWNTs-OH

The resulting MWNTs-COCl were mixed with 80 mL of ethylene glycol in the same 100 mL round shaped flask equipped with condenser and then magnetically stirred at 120 ℃ for 48 hours. The solid is filtered under vacuum and washed with anhydrous THF for several times until the solid is free from ethylene glycol (till the filtrate is colorless). Then the solid was dried in an oven at 105 ºC for 48 hours, yielding MWNTs-OH.

Characterization: FTIR, SEM, TEM, TGA, Elemental analysis and Solubility tests.

4.3. ATRP OF TERT-BUTYL ACRYLATE FROM MWNT-OH

Preparation of MWNTs-Br for ATR polymerization with t-butyl acrylate.

For the preparation of MWNTs-Br, 500 mg of MWNTs-OH are reacted with 2-bromo-2-methyl propionyl bromide (1.5 g) in the presence of $CHCl_3$(15 mL), triethylamine (1.0 mL, 14.3 mmol) and N,N dimethylaminopyridine (DMAP, 0.1 g, 1.64 mmol) at 0℃ for 1 hour, followed by reaction at room temperature for 48 hours.

Step-1

500 mg of MWNTs-OH is taken in two necked round bottom flask equipped with magnetic stirrer and sealed with stopper and to this 1.0 mL of triethylamine (14.3 mmol) , 0.1 gm of *N*,*N* dimethylaminopyridine (DMAP, 1.64 mmol) and most of chloroform (10 mL) are added. Then, this mixture was purged with nitrogen for 1 hour under stirring.

Step-2

In a glass tube 1.5 g of ATRP initiator i.e., 2-bromo-2- methyl propionyl is taken and the rest of chloroform (5 mL) is added, sealed with stopper, and flushed by nitrogen for 30 min.

The reaction mixture from the step-1 is cooled to 0 ℃ and the solution of ATRP initiator from step-2 was added into the reaction in a drop wise fashion for 60 minutes maintaining the temperature at 0 ℃. The mixture was then stirred for 1hour at 0℃ followed by stirring at room temperature for 48 hours. After 48 hours the reaction products are filtered under vacuum.

The collected solid is dispersed and washed with chloroform, then filtered under vacuum. This procedure of filtrand re-dispersion and filtration is done several times to ensure complete removal of initiator from filtrand. The filtrand black solid was collected and dried overnight in an oven at 40 ℃, resulting in MWNTs-supported ATRP initiator (MWNTs-Br). The synthesis procedure used for oxidation, diol spacer functionalisation and ATR polymerization follows the same way which were previously reported by Gao and coworkers [43,43a, 74].

ATR polymerization of *t*BA

A 100 mL dried two neck round bottom flask, equipped with magnetic stirrer and condenser was charged with 426 mg of MWNTs-Br, 80 mg (0.568 mmol) of CuBr, followed by the addition of 115 µL (0.544 mmol) of PMDETA and 8 mL of DMF. The flask was sealed with a rubber septum, and the contents were cooled to below 0 ℃ using liquid nitrogen and degassed and refilled with nitrogen three times (liquid reactants are solidified ,so that the degasification is

carried out in solid state without changing the concentration of reactants). After the addition of 8 mL (54 mmol) of deoxygenated *tert*-butyl acrylate via syringe, the flask was heated to 65 ℃ using oil bath for 24 hours (polymerization is carried under nitrogen atmosphere).

After 24 hours, the mixture was diluted in chloroform, vacuum filtered and washed with chloroform. The redispersion, vacuum filtration, and washing processes were repeated several times to ensure there was no ungrafted and free reagents mixed with the solid. The polymer modified MWNTs were dried in an oven at 40 ℃ for 2 4 hours.

Characterization: FTIR, SEM, TEM, TGA, and Solubility tests.

5. CHARACTERISATION AND DISCUSSION

5.1. OXIDATION, FUNCTIONALISATION, POLYMERISATION REACTIONS OF MWNTs

The oxidation of MWNTs was carried out in order to incorporate polar groups at the surface of these materials. The oxidation with nitric acid introduces carboxylic acids mainly but other functional groups are also formed such as lactones, phenol groups, quinones, Xanthene [58].

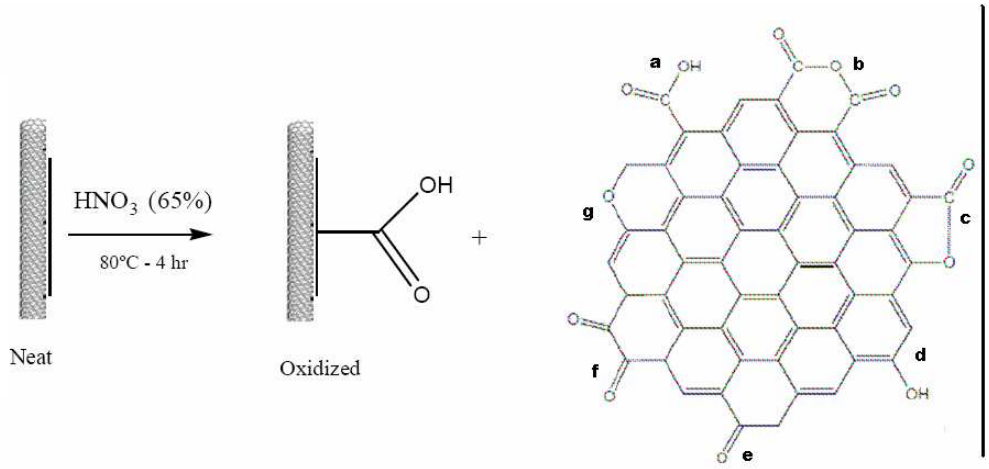

Figure-6: Nitric acid oxidation of MWNTs, a) Carboxylic acids groups, b) Carboxylic anhydride groups, c) Lactone groups, d) Phenol groups, e) Ketone groups, f) Quinone groups, g) Xanthene.

Carboxylic acid groups can be converted to acyl chlorides [74] using thionyl chloride. This can in turn, can react with ethylene glycol to produce an ester-alcohol, as illustrated in figure 7.

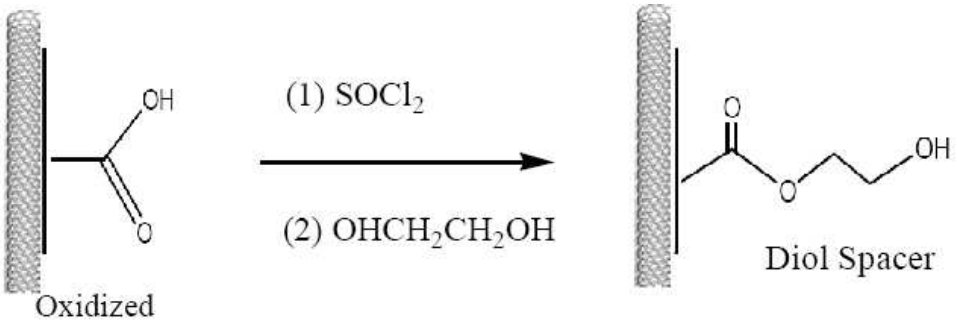

Figure-7: Diol Spacer functionalization of MWNTs

The MWNT-OH was further functionalized by esterification of the alcohol moiety by the ATRP initiator 2-Bromo-2-methylpropionyl bromide resulting MWNT-Br as illustrated in figure 8.

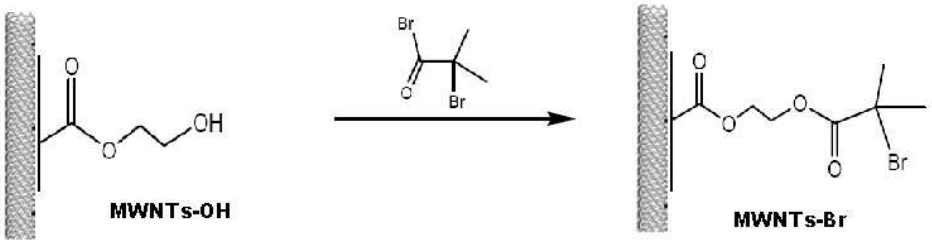

Figure-8: Anchoring of initiator to functionalized MWNTs (MWNT-OH)

The MWNT-Br was used as precursor for poly (tert-butyl acrylate)/MWNT materials using tert-butyl acrylate, as depicted in figure 9.

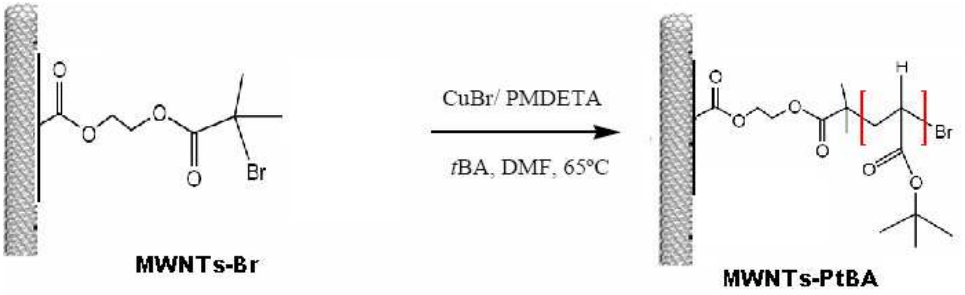

Figure-9: ATR Polymerization of *t*-Butyl acrylate.

5.2. SOLUBILITY TEST

Surface oxidation of MWNTs was carried out in order to incorporate polar groups at the surface of these tubes. Therefore, surface modification of the pristine MWNTs was monitored via solubility tests in water and toluene to assess modifications of the polarity of the functionalized tubes.

Figure-11 clearly shows the difference between the pristine MWNTs and oxidized MWNTs. MWNT-COOH, MWNT-OH, remain stable dissolved in water even after long periods (one hour). This was already noticed during filtration of the solution during treatments. The pristine MWNTs and MWNT-P*t*BA (ATRP polymerization) do not show affinity with water, being deposited at the bottom after some rest (10 min).

Figure-11: Water solubility test of all MWNTs

A-Pristine MWNTs

B-MWNT-COOH

C-MWNT-OH

D-MWNT-P*t*BA

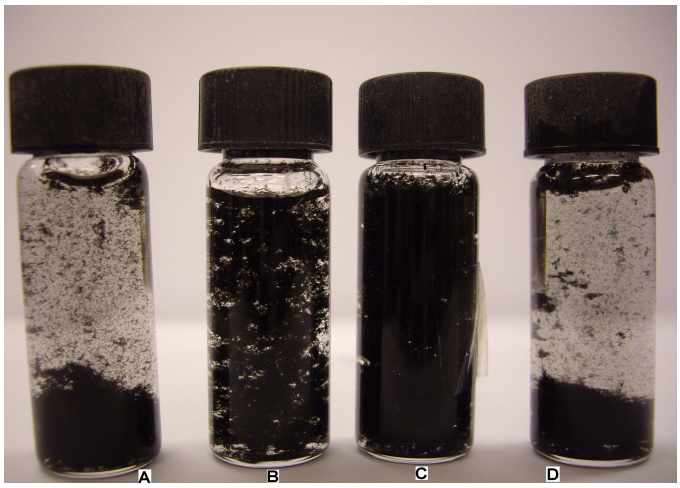

This behavior indicates that the functional groups attached to the surface of the tubes promote an increase on the polarity of the tubes. The presence of COOH, OH groups attached to its surface changed drastically the affinity of these tubes to polar structures. MWNT-PtBA which in principle is hydrophobic do not show affinity towards water but a slight amount of dispersion can be observed possibly due to the presenceof some residual tubes which have not been functionalized with PtBA.

Solubility tests in toluene were also carried out in order to differentiate oxidized MWNTs (MWNT-COOH) and MWNT-P*t*BA. From figure 12 clearly the difference between the tubes before and after functionalization can be observed. The dispersion of MWNT-P*t*BA remains stable in toluene even after 2 hours and MWNT, MWNT-COOH, MWNT-OH were not stable in toluene after the same period.

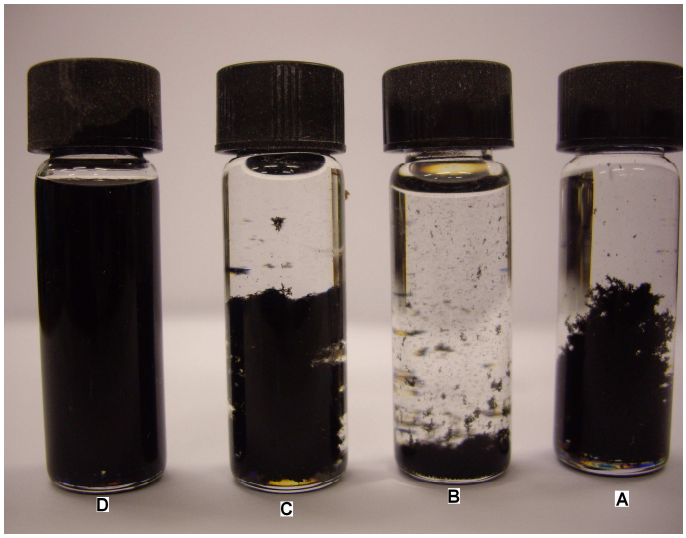

Figure-12: Toulene solubility test of all MWNTs

A-Pristine MWNTs

B-MWNT-COOH

C-MWNT-OH

D-MWNT-P*t*BA

In principle as the polymer is soluble in this solvent toluene, this dispersion also indicates the presence of polymer at the surface of the tubes promoting a better affinity with the solvent. The MWNT, MWNT-COOH, MWNT-OH do not present this behavior. All the acid functionalized tubes as well as the pristine MWNT do not disperse in toluene as expected

5.3. ^{1}H NMR SPECTROSCOPY

NMR analysis was conducted in order to identify *tert*-butyl acryltate characteristics resonances. The sample MWNT- P*t*BA is analyzed using proton NMR. This sample is dissolved in $CDCl_3$ and subjected to analysis.

According to Hao Kong [84] strong peaks at 1.43 and 2.21 ppm from tert-butyl groups and tertiary-carbon protons of P*t*BA should be present. From figure 13 ^{1}HNMR spectrum of MWNT- P*t*BA, these peaks are verified confirming the presence of polymer but the peaks from *tert*-butyl groups and tertiary-carbon protons are at 1.57 ppm and 2.18 ppm. These resonances indicate the presence of a polymeric structure, as they cannot be from graphite. The interaction with the MWNTs may have dislocated the peaks position.

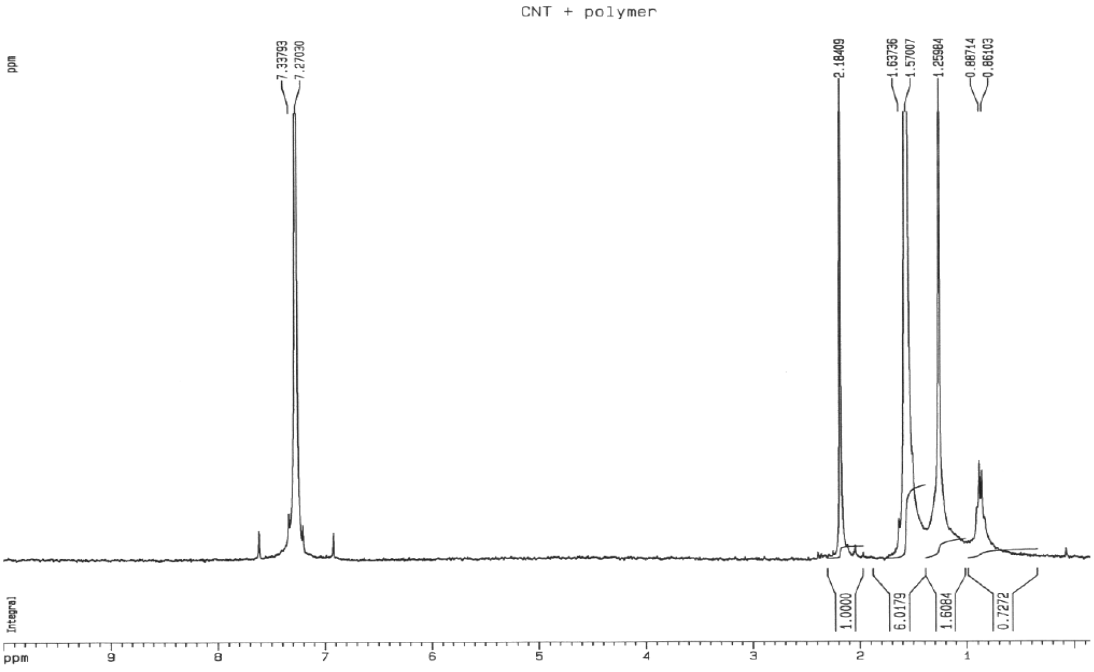

Figure-13: ^{1}HNMR Spectrum of MWNT-PtBA

5.4. INFRARED SPECTROSCOPY (FTIR)

MWNTs, MWNT-COOH, and MWNT-OH are subjected to FTIR spectroscopy but due to high aborptivity of the sample the spectrum cannot be obtained. From the FTIR spectrum of the MWNTs-PtBA, the absorbance of the expected C=O groups can be verified on 1720 cm^{-1}. A small peak at 2915 cm^{-1} indicates the presence of polymer and a broad peak at 1112 cm^{-1} also points out the presence of alcohols or carboxylic anhydrides that are from the poly (*t*-BA). The peak at 3405 cm^{-1} may be due to moisture or functional hydroxyl groups attached to the tubes surface. Carboxylic acid groups can also be present on the broad absorbance from 2800 to 3600 cm^{-1}[74b]. The spectrum of PtBA is added in the annex-1

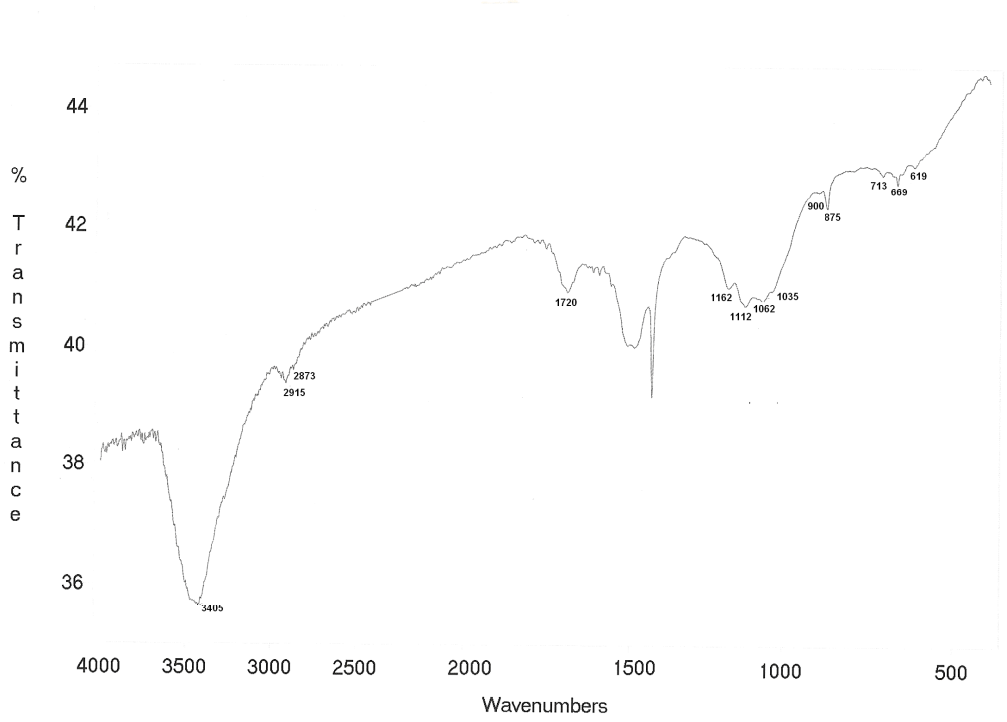

Figure -14: FTIR spectrum of MWNT-PtBA

5.5. ELEMENTAL ANALYSIS

The samples pristine MWNT, MWNT-COOH and MWNT-OH are subjected to elemental analysis the results are as follows.

Elements	MWNTs		Avg	MWNT-COOH		Avg	MWNT-OH		Avg
%Carbon	84.07	84.40	84.23	76.88	76.73	76.80	76.45	76.40	76.425
%Nitrogen	0.031	0.040	0.035	0.067	0.045	0.050	0.056	0.057	0.056
%Hydrogen	0.265	0.330	0.297	0.797	0.750	0.773	0.7 4	0.80	0.77
% Oxygen	100-(%N+%H+%C)= 15.438					22.377			22.749

Table- 5: Elemental analysis results.

From the above table it can be clearly viewed that the carbon amount decreased because of the treatment with acids. Nitric acid treatment resulted in the decrement of carbon concentration and an increment in hydrogen and oxygen concentrations, which suggested the presence of hydrogen and oxygen containing groups (COOH, OH).

5.6. EVALUATION OF THE THERMAL STABILITY

The thermal and thermo-oxidative stability of the pristine and functionalized MWNTs were studied. Both characteristics can be used as a rough estimation of the kind of functional groups that are present on the MWNTs surface. In fact, the functionalization method leads to different thermal and thermo-oxidative stability of the MWNTs.

The TGA results obtained for the pristine and the different functionalized MWNTs under nitrogen atmosphere are shown in figure 13(1). Pristine MWNTs are stable until 550 ℃ with no weight loss. The MWNTs treated with nitric acid (MWNTs-COOH) and diol functionalised (MWNTs-OH) start the degradation earlier mainly due to the loss of carboxylic acids and hydroxyl groups, since there is a weight loss around 400 ℃. This behavior is in line with the one observed by Chao Gao [74] in his studies.

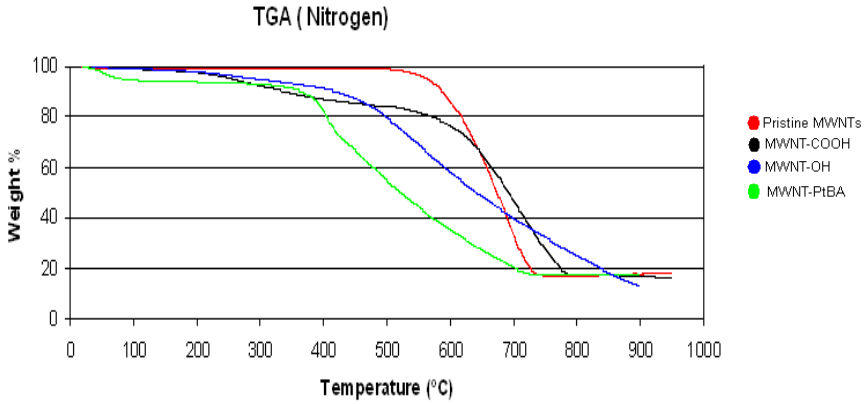

Figure-13 (1): TGA of MWNTs, MWNT-COOH, MWNT-OH, MWNT-PtBA under Nitrogen atmosphere.

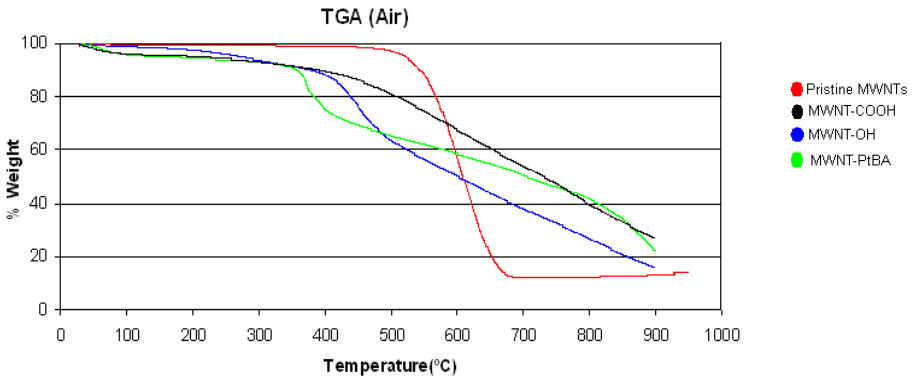

Figure-13 (2): TGA of MWNTs, MWNT-COOH, MWNT-OH, MWNT-PtBA under synthetic Air atmosphere.

Upon anchoring of the diol spacer the thermal stability of the material was further reduced since the decomposition for MWCNT-OH starts at 380ºC. As expected the polymerization process lowered the degradation temperature of MWNTs, this can be seen from the sample MWNT-PtBA. This is probably due to the presence of P*t*BA attached to the MWNTs surface. According to previous laboratorial analysis and from the literature [74b], the polymer decomposes from 200 to 400 º C. This can be clearly seen form the figure 13(1) that indicates the loss of polymer and second higher temperature represents the MWNTs degradation.

Similar differences were observed in the case of MWNTs samples analyzed under synthetic air atmosphere (figure-13(2)).In this case also, MWNTs-COOH and MWNT-OH started degradation earlier and this must probably due to functional groups attached to the MWNTs. In the case of MWNTs that were subjected to polymerization, earlier degradation is again due to the presence of polymer chains.

5.7. MORPHOLOGY STUDIES

The following images show the SEM micrographs of pristine MWNTs and diol functionalized MWNTs (Left-pristine, right–diol functionalized). The oxidation and functionalisation of MWNTs with diol did not produce significant changes on the morphology. All these samples show a relatively smooth surface and no changes in diameter of the tubes due to the surface treatments could be noticed.

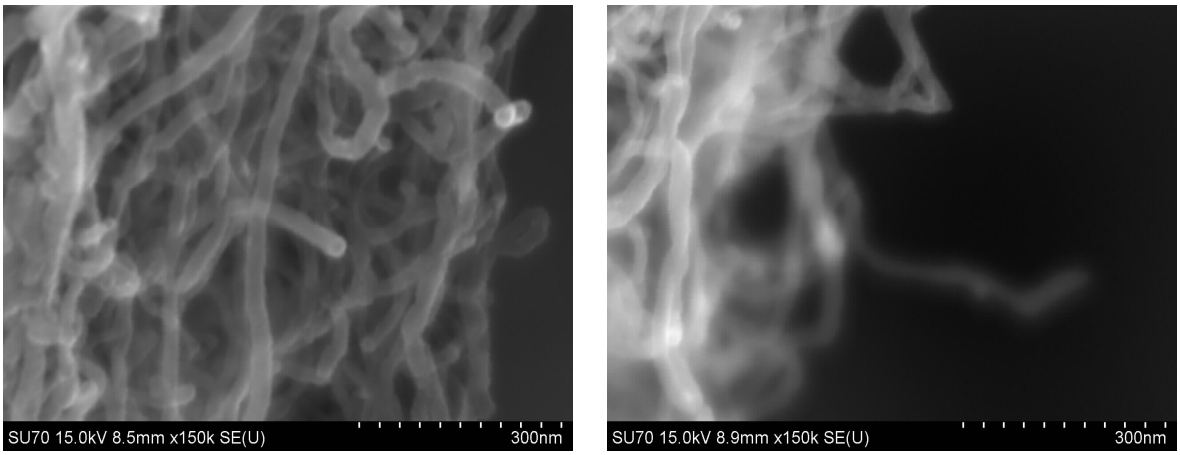

Figure-15: SEM micrographs of pristine (left) and diol functionalized MWNTs (right) at higher magnification

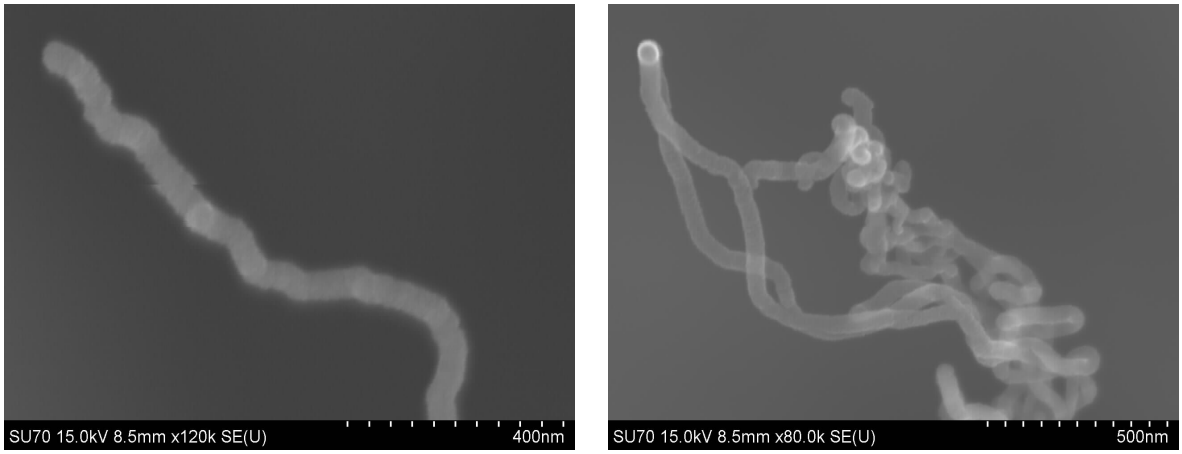

Figure-16: SEM micrographs of pristine (left) and diol functionalized MWNTs (right) at lower magnification

Even though the above images are at different magnification, it can be observed that the diameter as well as the roughness of the tubes are not changed after surface treatment of MWNTs.

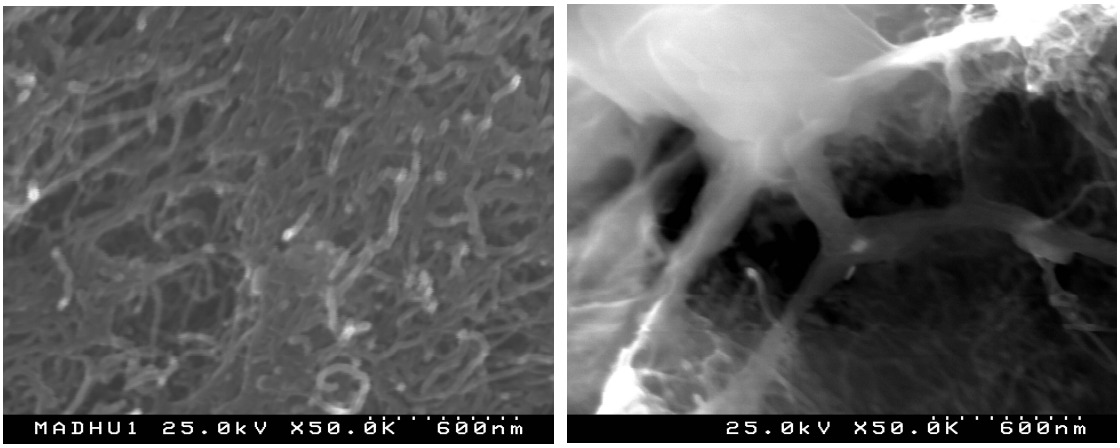

Figure-17: SEM micrographs of ATR polymerized MWNTs

The morphology of the MWNT-PtBA prepared by ATRP polymerization was studied by SEM. In the above image it can be verified clearly the presence of a polymeric film surrounding the MWNTs. This polymer shell is covalently bound to the tubes as it was not eliminated even after the filtration and several washings with chloroform.

From TEM micrographs, no significant differences are observed between the pristine and functionalized MWNTs (figure-18) but the difference can be observed between the pristine and ATR polymerized MWNTS (MWNT-PtBA).

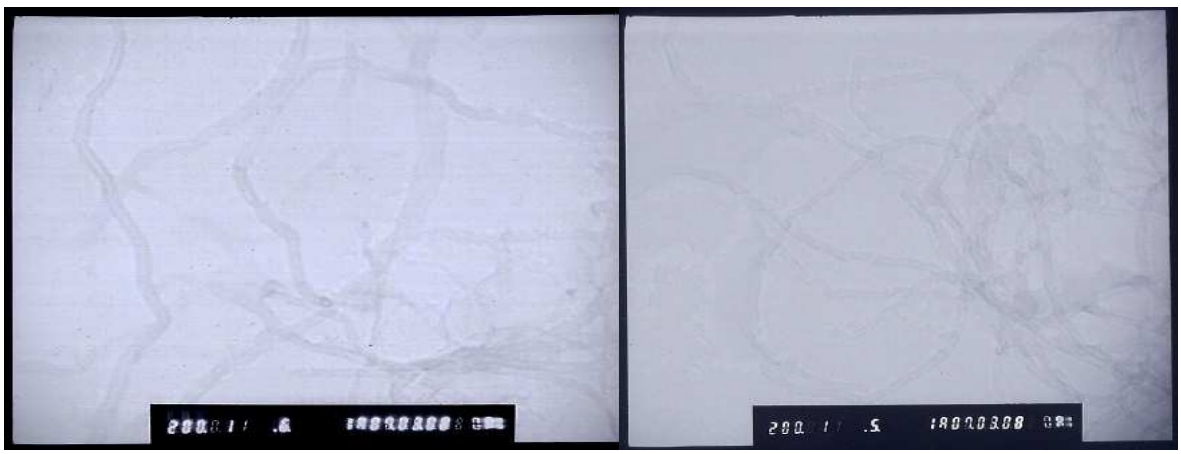

Figure-18: TEM images of pristine (left) and diol functionalized MWNTs (right)

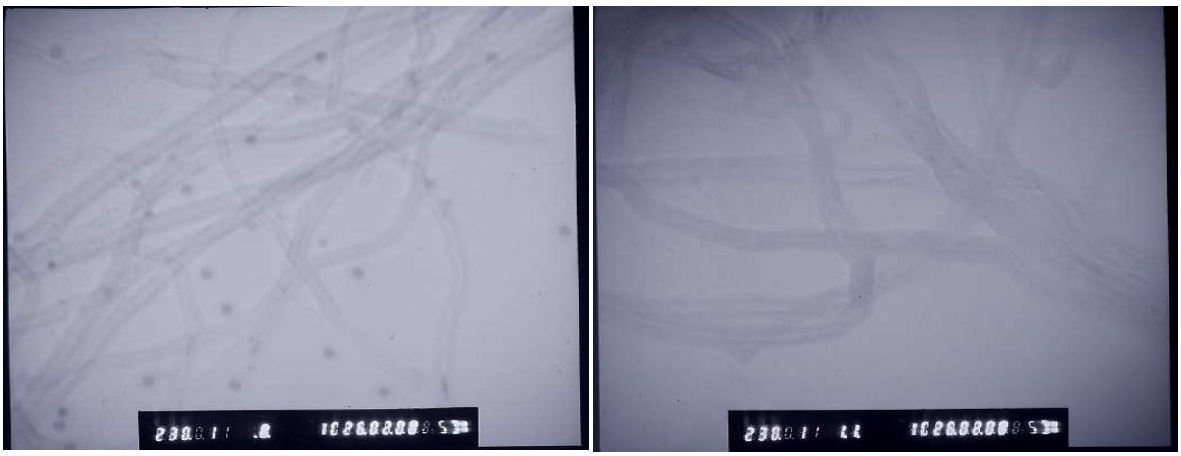

Figure-19: TEM images of pristine (left) and MWNTs-PtBA (right)

From the TEM images of MWNT-PtBA, at lower magnification it can be observed that the tubes are covered with the polymer shell. It may be stated that the polymer is covalently attached to the surface of MWNTs in a core shell structure, since after several washes of MWNTs-PtBA with chloroform ensures the complete removal of unbound PtBA.

CHAPTER III - CARBON FIBERS AND COMPOSITES

1. CARBON FIBERS

Carbon fiber also called graphite fiber is a material consisting of extremely thin fibers about 0.0002–0.0004 inches (0.005–0.010 mm) in diameter and composed of carbon atoms [10e]. The macro structure of crystalline carbon fibers shows that the graphite planes are oriented along the fiber axis and this helps to produce high modulus fiber. So, the CF produced in crystalline form have high modulus and can be considered for reinforcement purposes [10a]. Several thousand carbon fibers are twisted together to form a yarn, which may be used by itself or woven into a fabric. The density of carbon fiber is also considerably lower than the density of steel, making it ideal for applications requiring low weight. Carbon fibers (CF) have a unique combination of outstanding mechanical, physical and chemical properties, such as high strength, high modulus, high thermal resistance, low expansion coefficient and relative flexibility which makes them very popular in aerospace, military, motorsports and composites etc [10e].

The widely used carbon fibers are the high strength carbon fibers. Usually for these fibers the higher the modulus the lower the strength. Carbon fibers have better general properties than glass fibers and their price is much higher. Due to low thermal expansion of carbon fibre, carbon fiber reinforced composites have good dimensional stability.

2. CARBON FIBERS SURFACE MODIFICATION

Since carbon fibers have poor wettability and adsorption by most polymers, they exhibit low interfacial bonding strength with polymer matrices in CF composites and thereby good mechanical performance of composites can not be ensured. Several surface treatment techniques were developed to improve the wettability and interfacial adhesion of carbon fibers in polymer composites which includes plasma [87, 88], electrochemical oxidation [48, 49], wet chemical [89, 90] and thermal treatment [91-93].

2.1. CF SURFACE OXIDATION

Surface oxidation of CF improves the fiber surface wettability or increases the quantity of surface functional groups [94-98]. Oxidation methods consist of oxidizing the carbon fiber in a liquid or gas environment to form oxygen-containing functional groups such as carboxyl, carbonyl, lactones and/or hydroxyl groups on the surface of the fiber, while simultaneously increasing the surface area of the carbon fiber [97, 99-100, 108]. Thus the enlarged surface area enhances the interfacial bond the carbon filaments and the matrix by providing more points of contact/anchorage between the fiber and the matrix, or by enhancing the physicochemical interaction between the components [94, 98]. Though several studies are done in the area of surface treatment of CF using acids [101], no particular studies are dedicated to treatment of CF with only nitric acid followed by diol functionalization to generate strong adhesion between the fiber surface and matrix to improve the stress transfer from the relatively weak and compliant matrix to the strong and stiff reinforcing fibers.

3. POLYMERIC MATRIX

The polymeric matrix used in polymer composite materials can be from thermoplastic or from thermosetting resins. In the present work the epoxy resin (thermosetting resin) is used as matrix.

3.1. Epoxy Resins:

Epoxies were introduced independently, by Ciba AG in1943 and the Devoe and Reynolds Co. in 1950 [102]. This polymer fundamentally defines as thermosetting resins in which the cross-linking is derived from reaction of epoxy groups (the epoxy group is also called the epoxide).

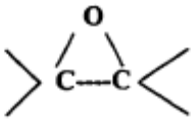

Figure- 20: Epoxy group

Presently up to 90% of commercial epoxy resins are made by the reaction of bisphenol A and epichlorhydrin [102] and the chemical structure of this resin can be seen in the figure 21.

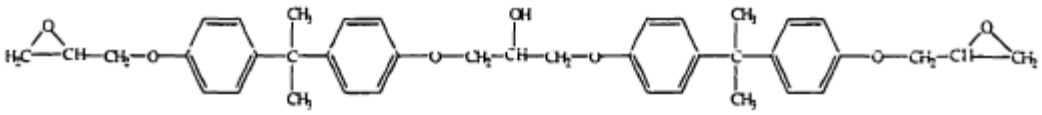

Figure-21: Chemical structure of epoxy resin

Epoxies can be cured by various kinds of materials such as polyamines, polyamides, polysulfides and urea and phenol formaldehyde through coupling or condensation reactions [103]. In general amine is one the most practical curing agents for initiating the epoxy chain reaction. Epoxy resins have good chemical and mechanical properties such as flexibility, adhesion, low shrinkage during curing, and environmental resistance, which make them suitable candidates for fiber reinforced composite materials.

4. INTERFACES IN FIBER REINFORCED POLYMER COMPOSITES

The fiber/matrix interface serves to transmit stress from the matrix to the reinforcing fibers and, in certain cases, to protect the fibers from stress corrosion, solvent contamination and general property deterioration. The interfacial properties also influence the crack propagation in a composite and therefore the macroscopic mechanical properties of fiber composites, such as strength and toughness, are also controlled by the fiber/matrix interface. In other words the overall performance of the composite materials depends on the strong interface in these materials.

The most important failure mechanisms in a fiber reinforced composite are the fiber pull out and debonding at the fiber/matrix interface. When there exists a strong interfacial bond between the matrix and reinforcement, the reinforcement strengthens the matrix. A mechanical bond is formed due to shrinkage of the polymeric matrix when the composite cools down from the processing temperature. In the case of high matrix shrinkage, residual stresses can be created both around the fiber and in the matrix. Therefore the matrix may be unable to transfer the stresses efficiently to the fibers due to mechanical bonding disruption at low stresses and the fiber/matrix interface debonding.

Figure 23 gives a basic idea of the interface in composite materials.

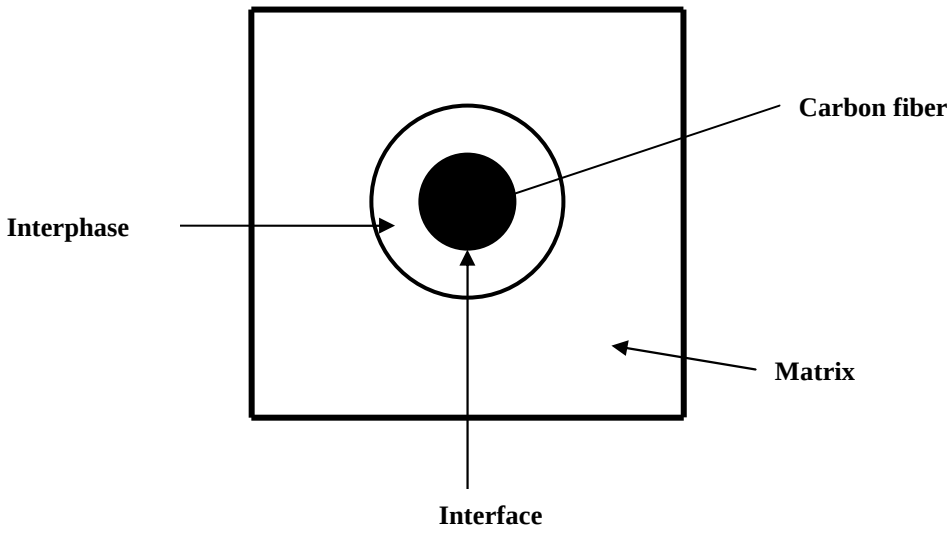

Figure-23: Interface in composite materials [104, 105].

Interphase: Interphase is defined as the 3-dimensional interfacial region of finite volume between the fiber and matrix with physical and chemical properties differing from those of the fiber and matrix respectively [104,105].

Interface: Interface is defined as a 2-dimensional border between the fiber and the interphase or the 2-dimensional border between the fiber and matrix if the interphase is not present [105].

The following factors contribute to the adhesion between fiber and matrix [106,107].

a) Mechanical interlocking because of surface morphology (surface roughness and micro porosity)

b) Chemical bonding due to functional groups present on reinforcement fiber (covalent bonding and acid-base interactions)

C) Physico-chemical interactions between the matrix and fiber (dispersive forces and dipole dipole interactions)

5. RAMAN SPECTROSCOPY

This part provides a short review of Raman spectroscopy to study the fiber/matrix interface in composite materials. First of all, the basic concepts of Raman scattering theory are presented. Afterwards, Raman spectra of carbon fiber and epoxy resin are briefly described.

In 1928 C.V. Raman discovered the inelastic scattering phenomenon which bears his name [128]. For his work on light scattering Raman was awarded the Nobel Prize in Physics in 1930. In Raman scattering, the frequency of the incident and scattered photons are different, and the difference is related to vibrational and/or rotational properties of the molecules from which the scattering occurs. Although the Raman Effect has been known for a long time, it has become an essential analytic tool in the last decades since powerful (monochromatic) laser sources could provide the impinging photon energies necessary to observe Raman scattering with a good signal to noise ratio [132].

Raman spectroscopy has found a wide range of applications. A typical application of Raman spectroscopy is the chemical identification of substances, their quantitative analysis, and the determination of their molecular structure [129]. In medicine, it is possible to use the Raman technique for real-time monitoring of anesthetic and respiratory gas mixtures during surgery [130]. In solid state Physics, Raman spectroscopy is used to characterize materials, find the crystallographic orientation of a sample, but also to study the electron-phonon interactions, the phonon density of states, or more specifically to determine the topological and geometrical parameters of sample [129,130]. Finally, this tool has found some application in remote monitoring for pollutants [131].

5.1 RAMAN SCATTERING THEORY

When the sample is irradiated by light, the molecules of matter interact with the photons. The interaction between matter and light can be interpreted as a collision between a vibrating molecule (or a phonon in a crystal) and an incident photon. As a result the scattering of light by the molecular system can be observed.

The predominant type of scattering is elastic scattering, called Rayleigh scattering. The energy of the elastic scattered photon as well as the energy of the molecule does not change after the collision. However, a small fraction of light (approximately 1 in 10^7 photons) is inelastically scattered. Such inelastic scattering is known as Raman scattering. The energy difference between the incident photon and the Raman scattered photon is equal to the energy of a molecular vibration.

If the vibrational energy of the molecule in the ground state is increased, and the energy of the scattered photons is decreased by the same amount, the type of scattering is called Stokes Raman scattering. On the other hand, if the molecule in the excited state loses energy, and the scattered photons gain energy by the same amount, the type of scattering is called anti-Stokes Raman scattering.

The energy level diagram for Rayleigh and Raman scattering is illustrated in figure 24

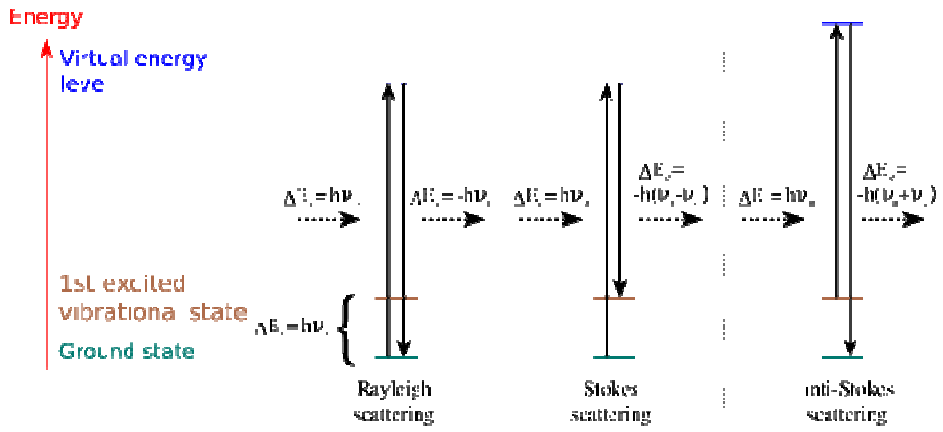

Figure-24: Energy level diagram for (a) Rayleigh scattering, (b) Stokes Raman scattering and (c) anti-Stokes Raman scattering [128].

The change in energy is proportional to a change in frequency [110]. Therefore, the spectral analysis of the scattered light shows an intense spectral line (Rayleigh line) matching the frequency of the incident light (υ_o). Additionally, weaker lines are observed at frequencies which are shifted compared to the frequency of the incident light. These lines shifted to lower (υ_o-υ_m) and higher (υ_o+υ_m) frequencies are known as Stokes and anti-Stokes Raman lines, respectively [111]. A schematic representation of Rayleigh line and Raman lines is shown in figure 25.

Since the Stokes Raman lines and anti-Stokes Raman lines gain and lose the same amount of energy, they are equally displaced with respect to the Rayleigh line, and contain the same frequency information. However, the anti-Stokes lines are much less intense than the corresponding Stokes lines. This occurs because anti-Stokes lines arise from the ground vibrational state and Stokes lines arise from the excited vibrational state. For this reason the more intense Stokes line is normally measured in Raman spectroscopy.

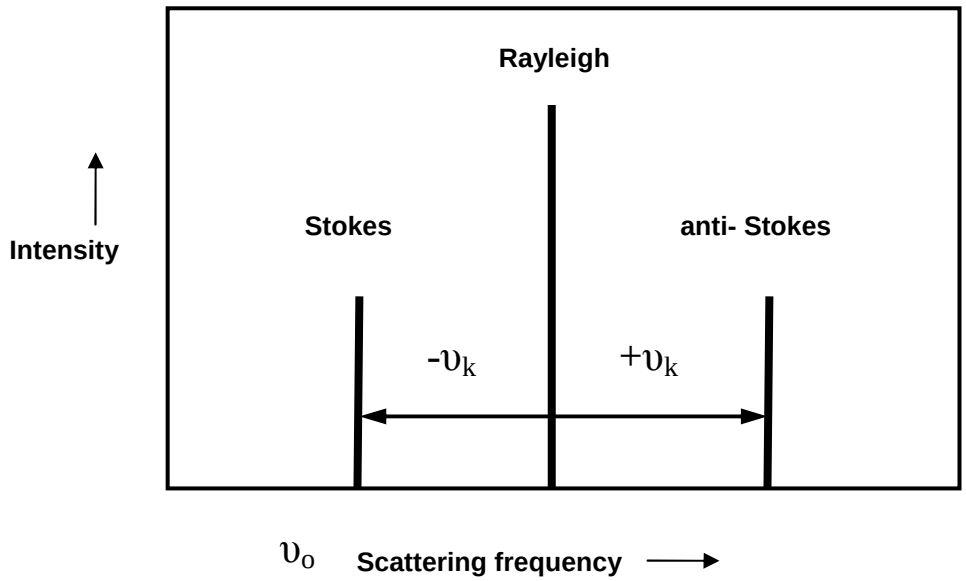

Figure-25: Schematic representation of Stokes Raman line, Rayleigh line and anti-Stokes Raman line [111].

As the Raman scattering phenomenon is very weak, a high power excitation source is necessary. Moreover, the excitation source should be monochromatic to facilitate Raman measurement. The lasers meet all these requirements [105].

5.2. RAMAN SCATTERING IN CF & EPOXY RESIN

In recent years Raman spectroscopy has emerged as a powerful technique for the characterization and identification of the various forms of carbon. Carbon can exhibit different arrangements in the solid state, such as the well known graphite and diamond structures, as well as more recently discovered structures based on fullerenes, CF and carbon nanotubes [112]. Each one of these carbon based materials yields a characteristic Raman spectrum.

Raman spectroscopy can also provide information about chemical composition, segmental orientation, conformation distribution, and phase identification for polymer systems [112].

5.2.1. RAMAN SPECTRA OF CF

The Raman spectroscopy of a high modulus polyacrylonitrile (HM PAN) based carbon fiber is described in this section. This fiber consists of a thin crystalline skin layer with a high orientation degree of the graphitic basal planes and a core with randomly oriented crystallites

[110]. Most of the Raman intensity of a carbon fiber will originate from this thin surface layer [113]. This aspect allows investigation of the carbon fiber composite using Raman Spectroscopy. A schematic representation of a PAN based carbon fiber and its graphite crystal structure in the surface layer is illustrated in Figure 26 (a) and Figure 26 (b).

The Raman spectrum of a high modulus PAN based carbon fiber in the region from 0 cm^{-1} to 3000cm^{-1} is shown in Figure 27. As seen from this figure, there are three major Raman active modes which are the double degenerate E_{2g2} mode of the graphite crystal at 1580 cm^{-1} (G line) and the first and second-order A_{1g} modes at 1330 (D line) and 2660 cm^{-1}(G' line) respectively. The A_{1g} modes cannot be defined from group theory, but they are attributed to be connected to either the breaking of the molecular symmetry in 'disordered' carbons or the presence of the exposed graphitic edge planes at the fiber surface [114].

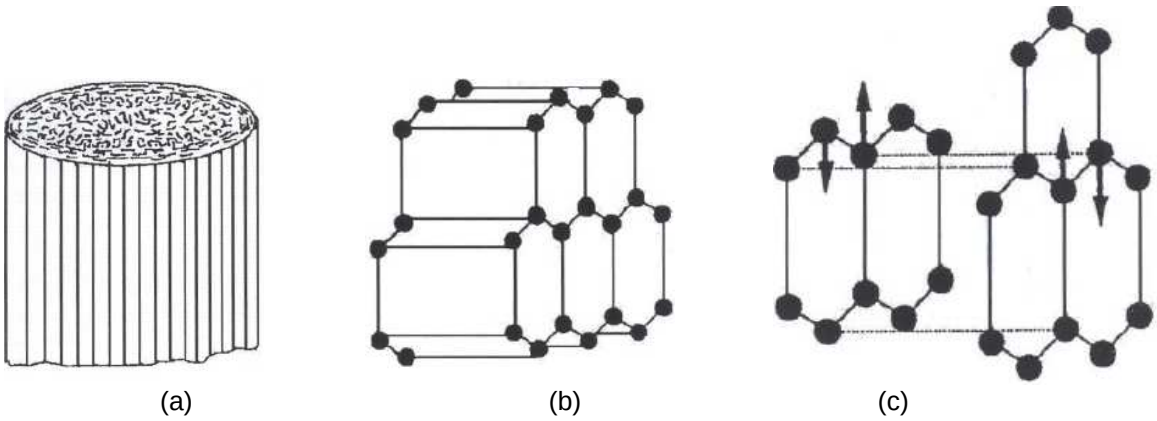

(a) (b) (c)

Figure-26: Schematic representation of (a) PAN based carbon fiber, (b) its graphite crystal structure in skin layer, and (c) in-plane E_{2g} vibration of the graphitic cell.

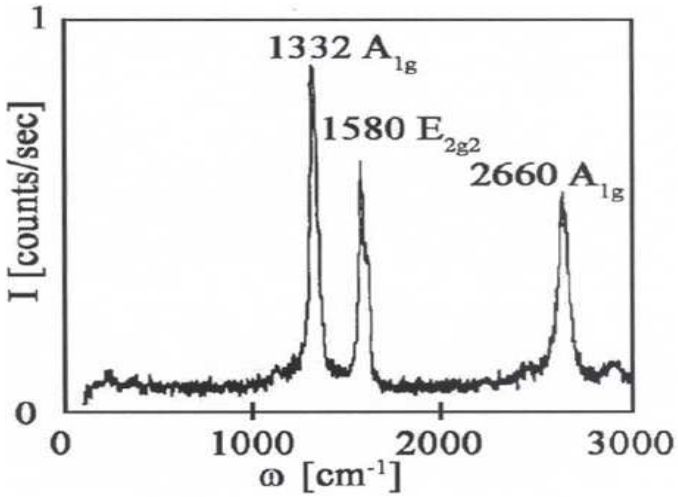

Figure-27: Raman spectrum of high modulus PAN based carbon fiber [110].

The band at 1580 cm^{-1} frequency is ascribed to the double degenerate deformation mode of the hexagonal ring structure having E_{2g} symmetry which has been observed in graphite [113]. The G line has been assigned to the stretching of the C-C bonds in the fiber due to the in-plane E_{2g} vibration of the graphitic cell as shown in Figure 26 (c). The first-order A_{1g} modes at 1330 cm^{-1} is not observed in Raman spectra of graphite single crystals, but it appears in all disordered forms of carbon [113]. The presence of the D line is thought to be due to the breakdown of the translational symmetry, caused by the crystal boundaries of the graphite [115]. The second-order A_{1g} modes at 2660 cm^{-1} frequency indicates the graphitization degree of the carbon fiber surface, what is confirmed by an increasing intensity of this peak with increasing graphitization [110]. The Raman band at 2660 cm^{-1} is thought to be a second-order band since it is found about twice the wave number of the 1330 cm^{-1} band [115]. The G' line tends to become sharper and more well defined as the fiber modulus increases because of the larger, better-oriented crystals [115].

The basic principle that allows using Raman spectroscopy for measurement stress in carbon-fiber reinforced composites is the strain dependence of certain vibrational modes of carbon fibers [114]. This technique is based on the fact that the interatomic frequencies which determine the atomic vibrational frequencies are inversely related to the interatomic separation. Thus, when the fiber is under the action of a tensile stress, the bond lengths are increased and the vibrational frequencies are decreased. When the fiber is under the action of a compressive stress a reverse effect is observed [116]. Therefore it has been found that all strain-sensitive bands in the carbon fiber spectra shift to lower frequency when the fiber is subjected to tension, and shift to higher frequency when it is subjected to compression. The peak position dependence of the 2660 cm^{-1} Raman band for a carbon fiber subjected to both tension and compression upon strain is shown in Figure 28. The dependence of the strain sensitive band position on strain was found to follow a linear relationship up to fiber fracture [115].

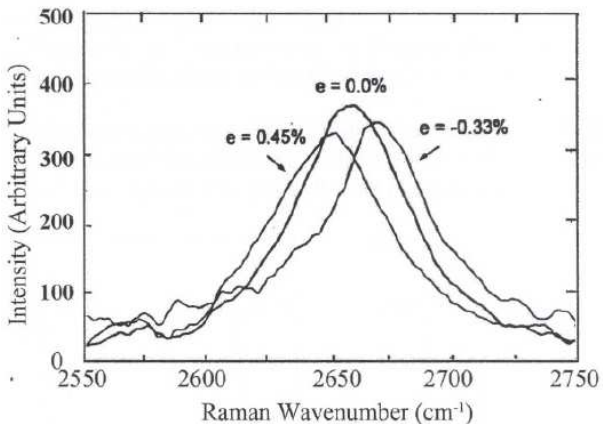

Figure-28: Strain-induced shift of the 2660 cm^{-1} Raman band for carbon fiber subjected to both tensile and compressive deformation [115].

The axial strain dependence of the D, G and G' spectral lines of a high modulus carbon fiber under tension was performed by Galiotis and Batchelder [113]. In their works sensitivity to strain of the double degenerate E_{2g2} mode corresponds to the value of -9.1 cm^{-1}per % strain. Additionally, strain dependence values of -7 cm^{-1} per % strain and -24 cm^{-1} per strain % for the first and second-order A_{1g} modes were measured, respectively. It is necessary to achieve the highest strain sensitivity to perform Raman spectral measurements. Therefore, the G' spectral line should be of interest to Raman investigation of carbon fiber since this band exhibits strain sensitivity almost twice higher for lower intensity and broader bandwidth than the G line [117].

5.2.2 RAMAN SPECTRA OF EPOXY RESIN

A considerable amount of Raman activity throughout the spectrum is demonstrated in the epoxy resin. However, the 1620 cm^{-1} line which is attributed to phenyl ring stretching vibration interferes with the Raman spectrum of the carbon fiber. In order to minimize the contribution of the resin Raman peak in the spectrum of the carbon fiber, confocal Raman spectroscopy should be used [114].

6. MATERIALS & EQUIPMENTS

6.1 CF & EPOXY RESIN

The ability of the interface to transfer load in fibrous composites is known to play an essential role in their performance. It is common practice to cover the fibers after production with a layer of protective sizing. The sizing of carbon fiber usually consists of a thin layer of epoxy resin which protects the carbon fiber surface and enhances the interfacial properties.

The materials used in the present work are unsized PAN based HM carbon fibers. The matrix was an epoxy resin based on the bisphenol group with a low molecular weight.

Material	Tg (℃)	Tensile Modulus (GPa)	Tensile Strength (MPa)	Tensile Elongation (%)
LM E20	70-95	3,0	70	4-6

Table-6: Epoxy properties provided by LM Glasfiber

Fiber Grade	Filament Diameter (μm)	Density (g/cm^3)	Tensile Strength (MPa)	Tensile Modulus (GPa)	Elongation (%)
Toho Tenax HM35	6,7	1,79	3240	345	0,9

Table-7: Carbon fiber properties provided by Toho Rayon

6.2. REAGENTS

HNO_3 (65%), $SOCl_2$ (99%), were purchased from Merck. Ethylene Glycol was purchased from Sigma chemicals, epoxy resin (LM E20) and hardener (LM-H20) were supplied by LM Glas fiber.

6.3 EQUIPMENTS

Raman spectra of samples were obtained using a Renishaw in Via Raman Microscopy fitted with a He-Ne laser giving monochromatic red light of wavelength 785 nm at an output power 17 mW. The laser was focused onto the fiber or matrix through a x 50 objective lens to obtain a laser spot in the range of diameter from 2 μm to 10 μm. The extended acquisition regime was employed to obtain the peaks position of the samples.

7. EXPERIMENTAL METHOD

7.1. SURFACE OXIDATION OF CF WITH HNO_3 (65%)

CF (amount as shown in table-8) were taken in a two neck round bottom flask equipped with reflux condenser and nitrogen inlet. Nitric acid (65 %) is added to this round bottom flask containing CF and the mixture is sonicated for 5 minutes at room temperature.

After sonication ensuring that the CF are well dispersed, the mixture is then heated (oxidized) in oil bath using a heating pan at 80 ºC for a specified time (table-8) with stirring (manually) under nitrogen atmosphere. Oxidation is carried out under nitrogen atmosphere as nitrogen acts as antioxidant gas and prevents oxidation of CF by atmospheric oxygen ensuring the oxidation is done, only by nitric acid.

After this, the remainents which are in acidic medium are neutralized by washing with distilled water and small amount of 0.1 N NaOH. The resultant oxidized CF are rinsed and filtered and then rinsed several times with distilled water to remove the neutralization products The oxidized CF in the solution (neutralized) were vacuum filtered and then subjected to drying at 105 ºC for 48 hours (till constant weight is attained).

The dried oxidized CF are characterized using SEM, LRS.

Table-8: Amount of MWNTs, acid used in each batch and process conditions used

Batch No.	Wt. of CF (Milligrams)	Nitric acid used (mL)	Sonificaion time (min)	Oxidation time (Hours)
1	20	20	3	1
2	20	20	3	2
3	20	20	30	--
4	20	20	15	--

Note- Samples 3 and 4 are only subjected to sonication in nitric acid.

7.2. FUNCTIONALISATION OF CF-COOH WITH DOIL SPACER (CF-OH)

Preparation of CF-COCl

Into a two neck round-shaped flask equipped with a condenser, 20 mg of CF-COOH were suspended in 15 mL of $SOCl_2$.The suspension was stirred at 65 ℃ for 24 hours. After 24 hours the remaining liquid was removed or evaporated under nitrogen flux at 40 ℃, leaving solid CF-COCl in the flask for further reaction.

Preparation of CFs -OH

The resulting CF-COCl were mixed with 80 mL of ethylene glycol in the same 100 mL round shaped flask equipped with condenser and then heated at 120 ℃ for 48 hours with stirring. The solid is filtered under vacuum and washed with anhydrous THF for several times until the solid is free from ethylene glycol (till the filtrate is colorless). Then, the CF was dried in an oven at 105 ºC for 48 hours, yielding CF-OH.

Characterization: SEM, LRS.

7.3. COMPOSITE SPECIMEN PREPARATION

A silicon form was used for fabrication of carbon/epoxy composites. An aluminium mould for production of silicon forms was filled by silicone and catalysis agent in a ratio of 20:1 respectively. The mould cured during night at room temperature. A silicon form and aluminium mould for its production can be seen in figure 29.

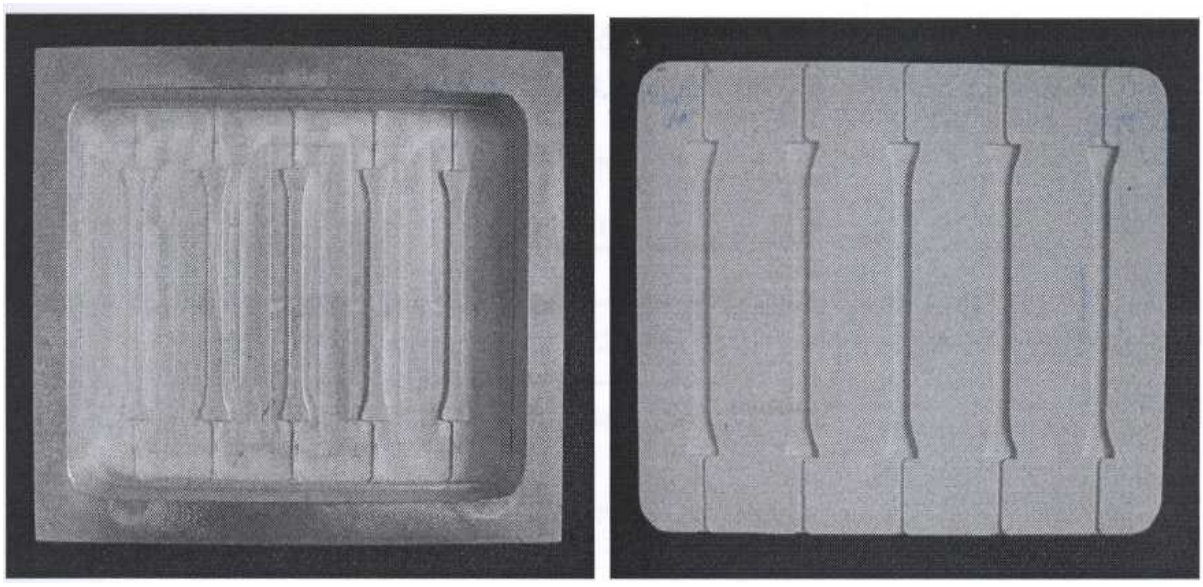

(a) (b)

Figure-29: (a) Aluminum mould for production of silicon form, (b) A silicon form for specimen fabrication.

The steps of the specimen fabrication are illustrated in Figure 30. The resin (LM-E20) and hardener (LM-H20) were mixed at room temperature in the proportion of 100:35 (%Wt.) After

mixing the epoxy and the hardener, the mixture was degassed during 20 minutes under full vacuum. Afterwards, a thin layer of epoxy resin with hardener was applied in a dog bone silicon mould then the individual short fiber was carefully aligned on the applied resin layer surface and then resin was again applied on CF filling the entire portion of mould. Finally the mould was put into a furnace. The samples were cured with heating rate and cooling rate 1℃/ min as shown in figure 31.

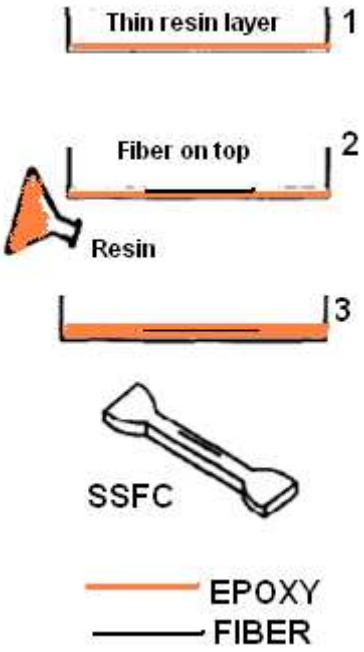

Figure-30: Specimen preparation for the short single fiber epoxy coupon [132].

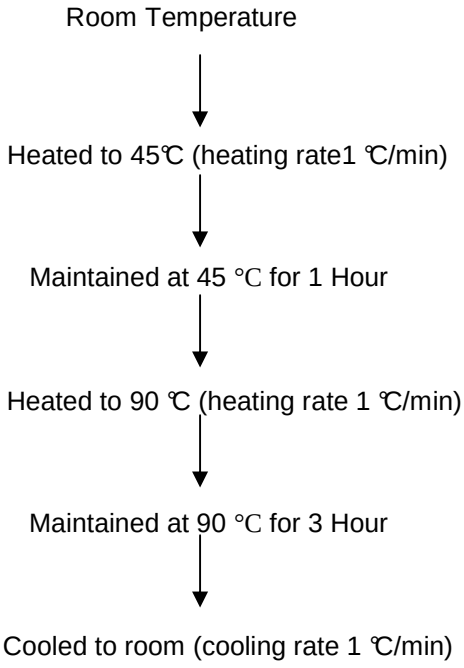

Figure-31: Curing cycle flow sheet

Figure 31(a) shows the specimen geometry. The dog bone geometry was chosen because it is the one required in order to use the tensile testing rig for in-situ Raman Spectroscopy analysis.

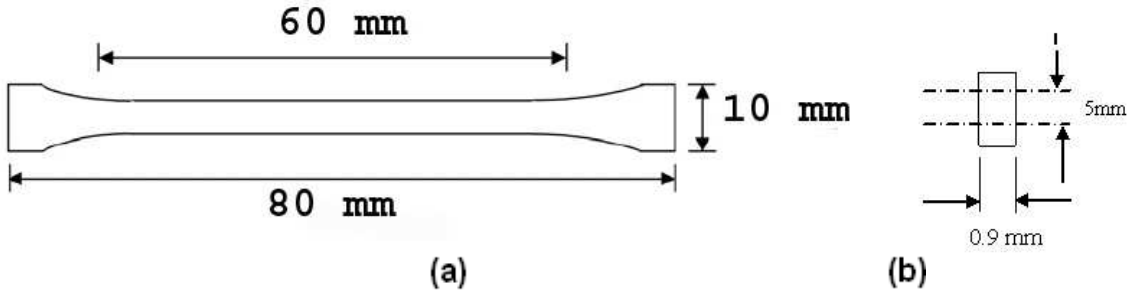

Figure-31(a): Final dimensions of a dog bone specimen (a) front view (b) side view [132]

7.4. COMPOSITE TESTING –TENSILE TEST INSITU RAMAN SPECTROSCOPY

The composite (dog bone shape) prepared using short single diol functionalized HM carbon fiber was subjected to tensile test, in which the single fiber CF/ epoxy composite specimen was mounted in the straining rig as shown in figure 32 (C). The working principle of the straining rig is similar to a normal tensile machine. It was special designed to fit in the Raman microscope. The straining rig has a linear displacement resolution of 4 µm per step. The static acquisition (covering the second-order region of the Raman spectrum i.e. in the range of 2660 cm^{-1}(G' line)) was used to determine the position of the peak corresponding to the applied deformation. The exposure time used for this Raman spectral acquisition was 40 seconds. The band intensity, band width and band position were obtained from static scans of the second-order Raman spectra and were fitted using Lorentzian band shape.

The applied tensile strain rate was 0.05 mm/min. Point-wise Raman measurements were taken along the fiber starting form the fiber end for each strain level. Laser Raman sampling was carried out in steps of 10 µm for the first 100 µm and 20 µm from 100 µm to 400 µm with load increment of 10 N per step until the matrix starts to yield.

Figure- 32: Raman Spectroscopy (A) equipped with a program (B) for examining the stress transfer between CF the polymer matrix using tensile testing rig (C) (the specimen color is modified using photoshop for better view)

8.0 MATERIAL CHARACTERIZATION & DISCUSSION

8.1. OXIDATION & FUNCTIONALIZATION REACTIONS OF CF

The oxidation of CF was carried out in order to incorporate polar groups at the surface of these materials. The oxidation of CF with nitric acid introduces carboxylic acids mainly but other functional groups are also formed such as lactones, phenol groups, quinones, xanthene [97, 99-100, 108].

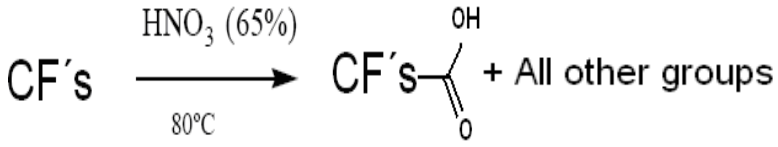

Figure-33: Nitric acid oxidation of CF

Carboxylic acid groups can be converted to acyl chlorides which in turn, can react with ethylene glycol to produce an ester-alcohol, as illustrated in figure 34.

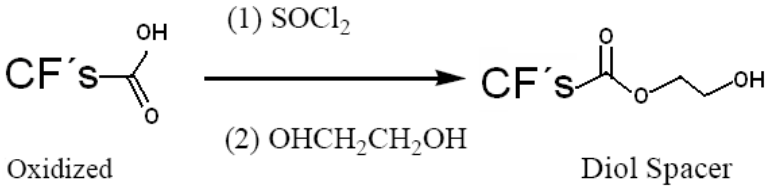

Figure-34: Diol spacer functionalization of CF

8.2. MORPHOLOGY STUDIES OF CF USING SEM

Carbon fibers usually perform a poor bonding behavior to polymer matrix due to their smoothness and their chemical inertness [109]. Various surface treatments like surface oxidation by acids, polymer coating, plasma activation, etc. can be used to improve the adhesion by chemical interlocking as a result of surface morphology.

In the present work the fiber surface was analyzed with Scanning Electron Microscopy (SEM). Due to good conductivity of the fibers, an additional coating layer was not required. The following figures 35 (a), (b), (c), show the surface morphology of treated and untreated CF.

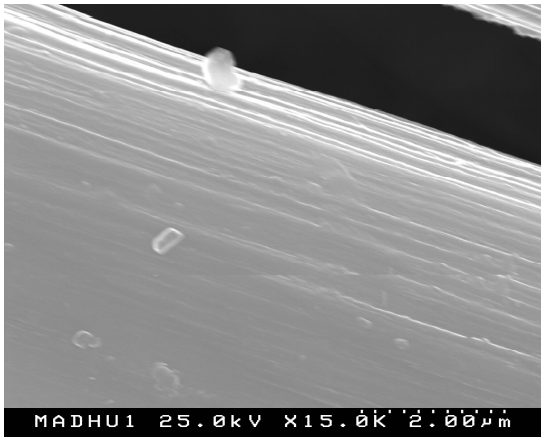

(a)

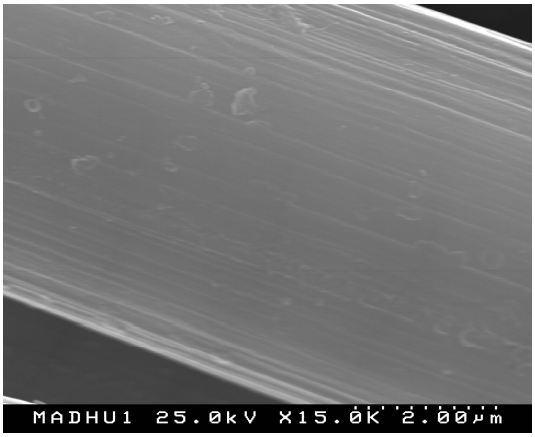

(b)

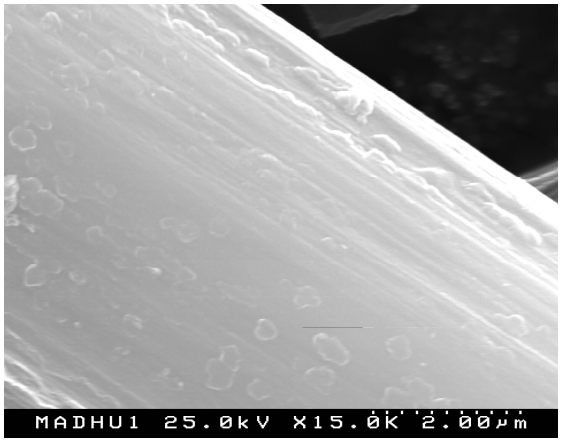

(c)

Figure-35: SEM images of carbon fiber:
(a) untreated desized CF
(b) diol functionalized CF (CF-OH)
(c) sonicated fibers (15 minutes)

All the samples were studied at the same magnification of 15000 times and compared. From the micrographs of the diol functionalized CF and untreated CF, no remarkable differences can be pointed out. In both the pictures the surface looks similar without any noticeable increase in the roughness, but the nitric acid treatment followed by diol functionalization may have surely produced changes in the surface properties that might not be able to differentiate using SEM as these changes may be very little or may be due to charging effects. Hence in order to have a clear view the untreated CF and CF-OH were subjected to Raman spectroscopic analysis. The presence of particles on the surface of the fibers can be external particles deposited during the handling of the fibers.

While in case of sonicated CF, increase in the surface roughness caused by acid etching can be easily observed. According to C.U. Pittmann Jr. et al., [97] this increased roughness is followed by the presence of acidic functions (carboxylic and phenolic hydroxyl groups) introduced on the carbon fiber's surface by nitric acid. Oxidation increases the total acidic functions simultaneously increasing the surface area (roughness).

This sonication procedure produced comparable surface roughness because of etching of fiber surface, but at the same time caused more damage to the fiber due to the strong effect of sonication. It is observed during the handling process of CF that these sonicated fibers were ultra brittle and difficult to handle in composite preparation.

8.3. SURFACE CHARACTERIZATION OF CF USING RAMAN SPECTROSCOPY

(Raman Spectra of carbon fibers)

Raman spectroscopy allows to differentiate zones with low, medium and high structural organization in carbon materials. The bands at or around 1350 cm^{-1} and around 1582 cm^{-1} are the main features of carbon materials and are called D bands (disordered) and G bands (ordered or graphitic), respectively. The ratio of intensities of D and G bands (I_D/I_G) can be regarded as a measure of the crystalline order of carbon materials [101].

Raman spectra of untreated and treated HM carbon fibers were obtained. The extended acquisition regime (in the range of 0 cm^{-1} of 3000 cm^{-1}) was employed to obtain the peaks position for both untreated and treated HM fibers. The exposure time used for this Raman spectral acquisition was 10 seconds and frequency peak values have been derived by applying Lorentzian fitting routines to the raw data obtained during Raman measurement. The following table shows the intensities of D, G bands and their ratio.

Table-9: Shows the intensities of D and G bands and their intensity ratio.

Raw Fiber	I_D	I_G	I_D/I_G
Point-1	9028.89	3751.96	2.4064
Point-2	7965.48	3313.84	2.4037
Point-3	8194.46	3300	2.4831
Point-4	8411.46	3496.84	2.4054
Point-5	8283.27	3287.82	2.5193
Diol Functionalized			
Point -1	11152.7	4230.30	2.6363
Point-2	13701.1	5125.83	2.6730
Point -3	13423.3	4281.77	2.7838
Point -4	13423.3	4769.83	2.6661
Point -5	10920.7	4083.83	2.6741
Oxidized – 2 hr			
Point -1	14341.3	5612.12	2.5556
Point-2	12341.4	4790.10	2.5764
Point-3	14212.8	5606.76	2.5349
Point-4	9867.18	3851.25	2.5620
Point-5	9774.64	3839.81	2.5456

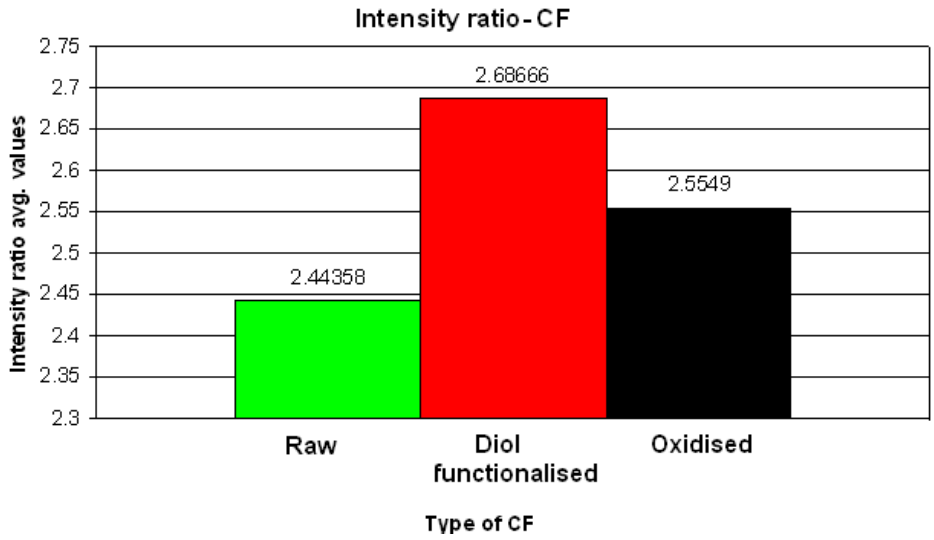

Figure-35(a): Average intensity ratio of different CF samples

The intensity ratio values of diol functionalized fibers (CF-OH) are higher than that of raw fibers, from which it can be stated that there is modification (or change in graphite structure) of the surface of diol functionalized carbon fiber sample. It is also observed from the above figure-35 that the intensity ratio values of diol functionalized CF are higher than oxidized ones from which indicates higher possibility of surface modification in diol functionalized CF. According to S.N. Chaudhuri et al. [118] the intensity ratio is directly related to the amount of ‘‘crystal boundary’’ in the carbon (graphite) fiber sample. A large amount of crystal boundary results in a higher probability of presence of functional groups (COOH, OH) after surface modification treatment and consequently, an increased interfacial shear strength between CF and epoxy matrix.

8.4. DETERMINATION OF RAMAN FREQUENCY GAUGE FACTOR (RFGF)

All strain sensitive Raman bands shift linearly to lower frequency under the tensile loading and to higher frequency under compressive loading. It is advantageous to have as great sensitivity to strain as possible for the Raman band frequency [113]. Hence in the present work the 2660 cm^{-1} peak was used for the strain measurements due to its high strain sensitivity. To perform strain measurements on a model composite, the strain dependence of the Raman frequency of a given vibrational mode on the applied tensile strain has to be determined [119].

To obtain a relationship between Raman frequency and tensile strain, a single fiber was stressed in air on the bending rig while Raman spectra were taken simultaneously for various strain increments. The bending rig consists of a clamp and a micrometer gauge. A single fiber was glued on a polymeric cantilever using araldite solution painted on its surface. Afterwards

the polymeric beam with the glued carbon fiber on the top was inserted into the clamp in the bending rig. The dial gauge is used to apply a known deformation to the cantilever beam, and according to the beam bending theory the strain in the fiber can be determined from the expression.

$$\varepsilon = \left(\frac{3h\delta}{2L^2}\right)\left(1-\frac{x}{L}\right)$$

Equation-2: For strain calculation in determination of RFGF

Where *h* is the height of the beam, δ is the deflection, χ is the distance from the clamped end to the point of Raman frequency measurement and L is the length of the beam. The bending rig is shown in the following figure 36.

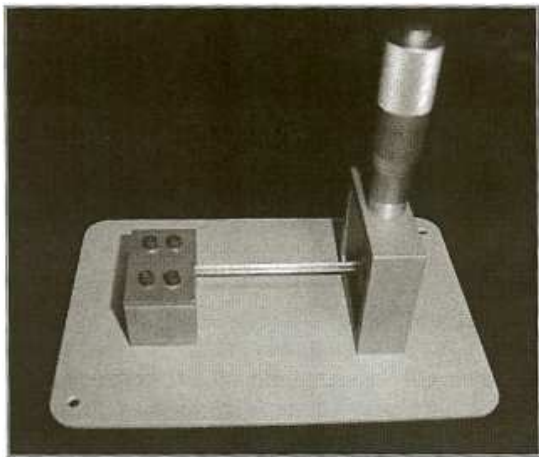

Figure-36: Showing the bending rig used for determination of RFGF.

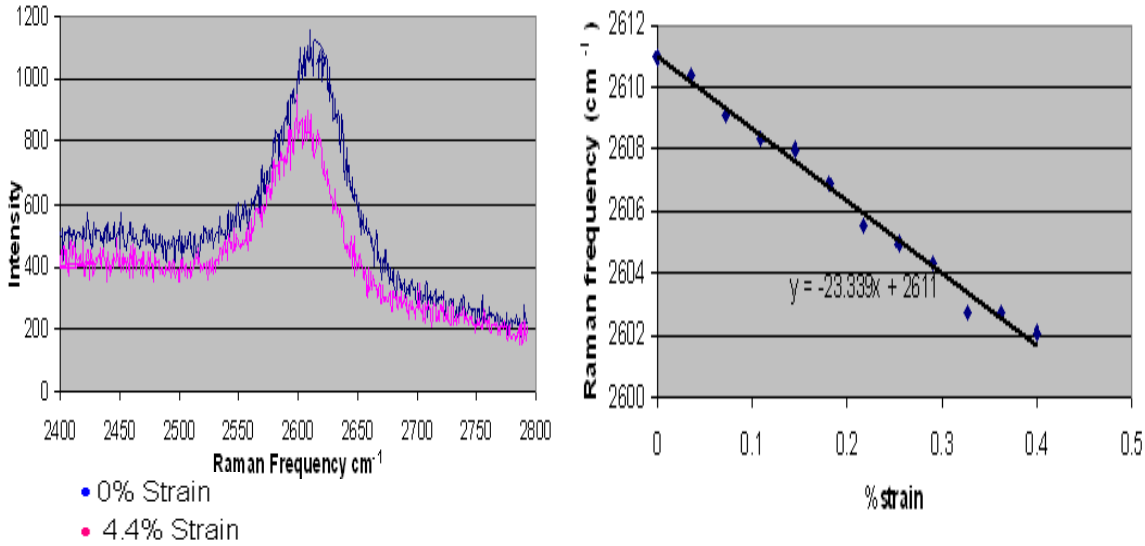

Figure-37: Shows (a) Strain-induced shifts of the 2660 cm^{-1} Raman band and (b) the strain sensitivity of the non-embedded HM diol functionalized carbon fiber subjected to tensile deformation.

The position of the Raman peaks for different values of applied strain (from figure 37(a)) were determined by using Lorentzian curve fitting method. Then from the known data of Raman frequency of different peaks at different applied strain values, a graph is drawn between Raman frequency of peaks at different levels of applied strain and applied strain % is drawn as shown in figure 37(b).

The curve was fitted to data with the least square method. The negative slope, plotted against Raman frequency and applied strain, of a least squared-fitted straight line represents the strain sensitivity S^{ε} of the carbon fiber and termed the Raman frequency gauge factor (RFGF) [120]. The strain sensitivity is described by equation 3.

$$S^{\varepsilon} = \left(\frac{\Delta \nu}{\Delta \varepsilon} \right)$$ Equation-3: For determination of RFGF

Where S^{ε} represents Raman frequency gauge factor (RFGF), ν is Raman frequency, ε is strain.

The slope of the straight line from the above equation gives the strain sensitivity S^{ε} of the carbon fiber and from the calculation it is determined as -23.339 cm^{-1} per % strain.

8.5. STRAIN MAPPING & DETERMINATION OF INTERFACIAL SHEAR STREANGTH

The first attempt to predict the interfacial shear stress in a single fiber composite was made by Cox. Shear lag model is used for the determination of interfacial shear stress and in this model it is assumed that both the fiber and matrix are elastic and perfectly bonded [3]. The final equation for the interfacial shear stress is as follows

$$\tau(x) = E_f(\varepsilon) \left(\frac{r}{2} \right) \left(\frac{d\varepsilon(x)}{dx} \right)$$

Equation-4: For calculation of interfacial shear stress

Where $E_f(\varepsilon)$ is the strain-dependent fiber Young's Modulus, ε is the axial strain, r is the radius of CF and x is distance along the CF.

Before applying the final equation for the determination of interfacial shear stress, the following steps were used for transformation of Raman spectroscopic data into % fiber strain.

(1) The Raman peak positions for different values of applied strain were determined using Lorentzian curve fitting method, similar to method applied for determination of RFGF.

(2) From the known values of frequency of stress free fiber (i.e. at unloaded condition) and stressed fiber (i.e. under loaded condition) and RFGF, equation-5 was used to determine the strain in the fiber.

$$\varepsilon_i = \left(\frac{\nu_i - \nu_0}{S^{\varepsilon}} \right)$$ Equation-5: For calculating fiber strain

Where ε_i is the strain in the embedded fiber at point i, ν_i, ν_0 represents the frequency of stressed and stress free fiber in air and S^{ε} is RMGF.

Then form the calculated values of fiber strain at different points along the length of the fiber for different applied strain values, a graph is drawn between the distance along the fiber and % fiber strain as shown in figure 38 and the slope of the curve was calculated and used in final equation (4) for determination of interfacial shear stress.

The strain profiles along the length of the short filament for different levels of strain (sample strain) are as shown in the following figure 38.

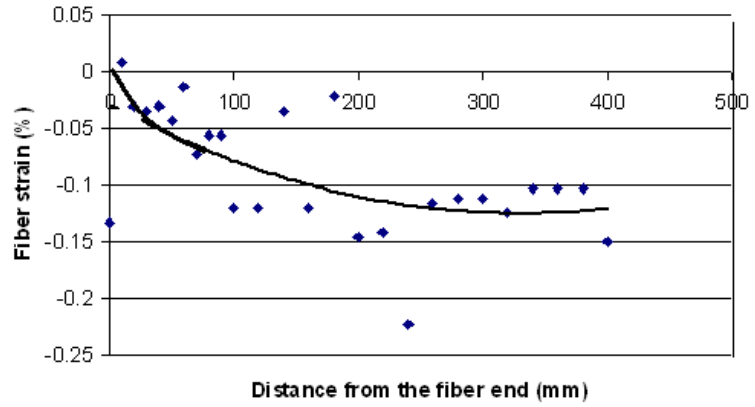

(1)

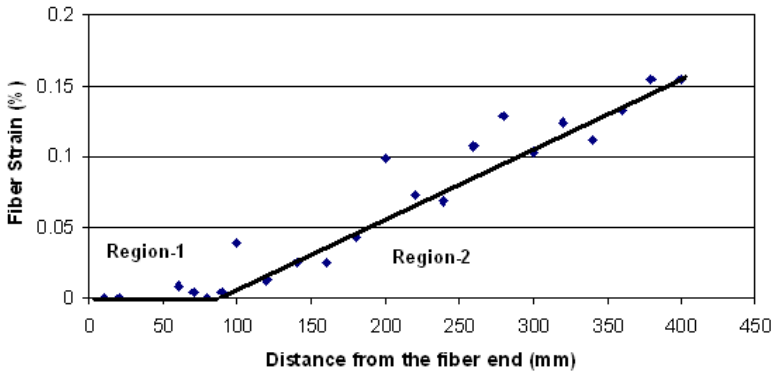

(2)

Figure-38: Showing the fiber strain distribution along the short HM CF-OH embedded in the epoxy resin at applied strain of (1) 0% (2) 1.3%

It can be seen from figure 38(1) that at 0% applied strain (under no load condition) the fiber strain values are in negative x-axis which indicates that the short fiber is under initial compressive strain of about 0.13% this is due to the compressive forces caused by resin shrinkage occurred during curing process of epoxy matrix. With the increase in the applied strain on the specimen the fiber strain builds from the fiber end and reaches to the maximum value towards to the middle of the fiber. From the strain distribution curve at 1.3% applied strain

(or sample strain i.e. at applied stress of 15.2 MPa , see annex-2: Stress- strain curve) it can be seen that the fiber strain curve fashion altered with one part of region (region 1) on x-axis indicating no load transfer situation and second region (region 2) shows linear increase in the fiber strain with applied load indicating the load transfer characteristics. Region 1 of the plot indicates that the debonding of the CF from the epoxy matrix has started, because of which there no load transfer between the matrix and fiber in this region and the linear fashion in region 2 describes the load transfer is because of friction between the fiber and matrix. Similar pattern was observed in the work of L.S. Schadler [121].

The Maximum value of interfacial shear stress (i,e interfacial shear strength) was calculated by determining the slope of line in region-2 (from figure 38 (2)). It was then applied in equation- 4 and the maximum interfacial shear stress was found to be 23MPa. This value was compared with interfacial shear strength of the unmodified HM carbon fiber epoxy composite, which was 40 MPa [121, 121a]. From these results, it was clear that the interface between the CF-OH and epoxy resin matrix was not as good as compared to that of pristine surface.

CHAPTER IV- FINAL CONCLUSIONS & CONSIDERATIONS

1. CONCLUSIONS ON MWNTs SURFACE MODIFICATION

Dispersion experiments showed that MWNTs treated with HNO_3 have good affinity for water because of the incorporation of alcohol groups. Solubility tests suggest the polymerization mechanism weren't 100% effective, which means that the polymer brushes didn't cover the whole surface area of the MWNTs. As a result, some of the submitted to polymerization remained soluble in water. After comparative tests in toluene however, there is a clear indication that an amount of tubes incorporated with P*t*BA brushes on their surface are comparable.

It is quite evident from the proton NMR result the presence of polymer brushes attached to the MWNTs. However, there is little shift in the resonance as expected due to the presence of the MWNTs. This is also clearly visible from the FTIR result of MWNT-PtBA, the position of peaks indicate that the presence of polymer and hence ATRP can be used for grafting poly tert-butyl acrylate chains from oxidized MWNTs.

Surface roughness and the average diameter of the tubes could not be exactly determined by the use of SEM or TEM. The differences between pristine and functionalized MWNTs were unable to differentiate using SEM and TEM. Trails are made to analyze the samples under increased magnification but at higher magnification there occurred the problems of continuous drift of the sample due to field effects. The SEM and TEM micrographs of MWNT-PtBA also indicate the presence of a continuous phase of poly (tert-butyl acrylate) surrounding the tubes.

The elemental analysis results of the pristine MWNTs, MWNT-COOH, and MWNT-OH also shows an increase in percentage of hydrogen and oxygen atoms which in turn indicates that there is an increase in hydrogen and oxygen containing groups. From this, it can be stated that the nitric acid treatment produces change in the surface of the tubes. From the TGA results, it is clearly visible that this surface modification process produced a change in the chemical nature of MWNTs. Functionalization and polymerization reactions resulted in the poor thermal stability of MWNTs because of the presence of COOH and OH groups on the MWNT-COOH, MWNT-OH and polymer in MWNT-PtBA.

Form the above results it may be stated that this functionalization & polymerization process can be applied for the surface modification of MWNTs and thereby in the production of MWNT-polymer composites with superior properties.

2. CONCLUSIONS ON CF SURFACE MODIFICATION & FUNCTIONALISED CF / EPOXY COMPOSITES.

In this part of the work, the same surface modification procedure used for MWNTs is applied for the surface modification of HM PAN based CF and the influence of this functionalization on the interface between the Cf and epoxy matrix was investigated.

The morphological studies were done using SEM, all the samples were studied at the same magnification of 15000 times and compared. From the micrographs of the diol functionalized CF and untreated CF, no remarkable differences can be pointed out it. While in case of sonicated CF, increase in the surface roughness caused by acid etching can be easily observed. Sonication resulted in more damage of the surface of CF and this process made the sample more brittle resulting the composite preperation difficult. Hence, the sonication process was not used in this present work.

The Raman spectra was used to characterize CF, CF-OH, CF-COOH. From the results of intensity ratios of D and G bands (table-9) it was evident that the diol functionalization modified the graphite structure on the suface of CF as compared to oxidation treatment.

Laser Raman spectroscopy has been used to measure the insitu strain in the CF-OH embedded in the epoxy resin matrix. Strain mapping was done form the data obtained from the test and the interfacial shear stress was determined form the Shear lag model. The maximum value of interfacial shear stress was found to be 23 MPa. This value was compared with interfacial shear strength of the unmodified HM carbon fiber epoxy composite, which was 40 MPa. From these results, it was clear that the interface between the CF-OH and epoxy resin matrix was not as good as compared to that of pristine surface.

The main reason for diol spacer functionalization is to promote better CF/ matrix interaction but, from the above result it can be seen that the functionalization of CF resulted in the low interfacial strength in CF/epoxy composite. The possible reason might be that this diol spacer functionalization process seems to make CF susceptible to absorb moisture (not actually but seems to be hydrophilic, the same was observed from solubility results of MWNTs) resulting in the negative effect at the interface. This moisture acts as a plasticizer at the interface interrupting the bonds between the CF and epoxy matrix (Covalent, Van der waals, London interactions) and thereby effecting the interfacial properties. Hence, might be because of this reason in this work the interfacial shear strength of the diol functionalized CF /epoxy is lower than unmodified CF/ epoxy.

REFERENCES

[1] S. Iijima, “Helical microtubules of graphitic carbon”, Nature 354 (1991) 56–58.

[2] Rodney S. Ruoff, Dong Qian, Wing Kam Liu, R. Physique 4 (2003), “Mechanical properties of carbon nanotubes: theoretical predictions and experimental measurements”, 993–1008.

[3] S.J. Tans, R.M. Verschueren, C. Dekker, “Room temperature transistor based on a single carbon nanotube”, Nature 393 (1998) 49–51.

[4] H. Dai, J.H. Hafner, A.G. Rinzler, D.T. Cobert, R.E. Smalley, “Nanotubes as nanoprobes in scanning probe microscopy”, Nature 384 (1996) 147–150.

[5] P. Poncharal, Z.L. Wang, D. Ugarte, W.A. de Heer, “Electrostatic deflections and electrochemical resonances of carbon nanotubes”, Science 283 (1999) 1513–1516.

[6] A.C. Dillon, K.M. Jones, T.A. Bekkedahl, C.H. Kiang, D.S. Bethune, M.J. Heben, “Storage of hydrogen in single-walled carbon nanotubes”, Nature 386 (1997) 377–379.

[7] L. Yukui, Z. Changchun, L. Xinghui, “Field emission display with carbon nanotubes cathode : prepared by a screen-printing process”, Diamond Relat. Mater. 11 (2002) 1845–1847.

[8] C.J. Lee, D.W. Kim, T.J. Lee, Y.C. Choi, Y.S. Park, W.S. Kim, Y.H. Lee, W.B. Choi, N.S. Lee, J.M. Kim, Y.G. Choi, S.C. Yu, “Synthesis of uniformly distributed carbon nanotubes on a large area of Si substrates by thermal chemical vapor deposition”, Appl. Phys. Lett. 75 (1999) 1721–1723.

[9] P. Kim, C.M. Lieber, “Nanotube tweezers”, Science 286 (1999) 2148–2150.

[10] P.G. Collins, K. Bradley, M. Ishigami, A. Zettl, “Extreme oxygen sensitivity of electronic properties of carbon nanotubes”, Science 287 (2000) 1801–1804.

[10 a] M.R. Piggott, “Load Bearing Fiber Composites”, Pergamon Press, (198G), 42-52

[10 b] K. Potter, “An Introduction to Composite Products”, Chapman & Hall, (1997), 64-87

[10 c] F.N. Cogswell, “Thermoplastic Aromatic Polymer Composites”, Butterworth Ltd

(1992) 33.

[10d] P.K. Mallick, “Fiber Reinforced Composites”, Marcel Dekker, Inc. (19931, Chapters: 1,2,5.)

[10e] http://en.wikipedia.org/wiki/Carbon_fiber

[11] Glushanin. S, Topolov. V. Y, Krivoruchko.A. V, "Features of piezoelectric properties of 0-3 PbTiO3-type ceramic/polymer composites", Materials Chemistry and Physics 97 (2-3), 357-364,(2006).

[12] Hine. P, Broome. V, Ward. I, "The incorporation of carbon nanofibres to enhance the properties of self reinforced, single polymer composites", Polymer 46 (24), 10936-10944, (2005).

[13] Cioffi. N, Torsi. L, Ditaranto. N, Tantillo. G, Ghibelli. L, Sabbatini. L, Bleve-Zacheo. T.D, Alessio. M, Zambonin. P. G, Traversa. E, "Copper nanoparticle/polymer composites with antifungal and bacteriostatic properties", Chemistry of Materials 17 (21), 5255-5262, (2005).

[14] Pelaiz-Barranco. A, Marin-Franch. P, "Piezo-, pyro-, ferro-, and dielectric properties of ceramic/ polymer composites obtained from two modifications of lead titanate", Journal of Applied Physics 97 (3) (2005).

[15] Huang. Z. M, Zhang. Y. Z, Kotaki. M, Ramakrishna. S, "A review on polymer nanofibers by electrospinning and their applications in nanocomposites", Composites Science and Technology 63 (15), 2223-2253, (2003).

[16] Jordan. J, Jacob. K. I, Tannenbaum. R, Sharaf. M. A, Jasiuk. I, "Experimental trends in polymer nanocomposites - a review", Materials Science and Engineering A-Structural Materials Properties Microstructure and Processing 393 (1-2), 1-11, (2005).

[17] Gerard. J. F, "Fillers and filled polymers", Wiley-VCH: Weinheim, (2001).

[18] Y.-H. Liao. O. Marietta-Tondin. Z. Liang, C. Zhang, B. Wang, Mater. Sci. Eng. A 385 (2004) 175–181.

[19] F.H. Gojny, K. Schulte, Compos. Sci. Technol. 64 (2004) 2303–2308.

[20] Ros. T. G, Van Dillen. A J, Geus.J, D, Koningsberger.C, “Surface Oxidation of Carbon Nanofibres”, Chemical European Journal, 2002.

[21]S.J.V. Frankland,A. Caglar, D.W. Brenner, M. Griebel,J. Phys. Chem. B 106 (2002).

[22] S. J. Park, B. J. Kim,“Roles of acidic functional groups of carbon fiber surfaces in enhancing interfacial adhesion behavior”, Mater Sci. Eng. A 2005; 408:269-74.

[23] S.P. Lin, J.L. Han, J.T. Yeh, F.C. Chang, K.H. Hsieh, “Composites of UHMWPE fiber reinforced PU/epoxy grafted interpenetrating polymer networks”, Eur Polym J 2007; 43:996-1008.

[24] H. Dvir, J. Jopp, M. Gottlieb, “Estimation of polymer–surface interfacial interaction strength by a contact AFM technique”, J Colliod Interface Sci. 2006; 304:58-64.

[25] Jang-Kyo Kim, Yiu-Wing Mai and Yiu-Wing Mai, “Surface treatments of fibers and effects on composite properties”, Engineered Interfaces in Fiber Reinforced Composites 1998, Pages 171-237

[26] M. A. Montes-Moran, A. Martinez-Alonso, J. M. Tascon, “Effects of plasma oxidation on the surface and interfacial properties of ultra-high modulus carbon fibres”, Compos Part A 2001; 32:361-6.

[27] J. P. Boudou, J. I. Paredes, A. Cuesta, A. Martinez-Alonso, “Oxygen plasma modification of pitch-based isotropic carbon fibres”, Carbon 2003;41:41-8.

[28] A. Fukunaga, S. Ueda, “Anodic surface oxidation for pitch-based carbon fibers and the interfacial bond strengths in epoxy matrices”, Compos Sci. Tech. 2000;60:249-59.

[29] H. Cao, Y. Huang, Z. Zhang, J. Sun, “Uniform modification of carbon fibers surface in 3-D fabrics using intermittent electrochemical treatment”, Compos Sci. Tech. 2005;65:1655-67.

[30] F. Severini, L. Formaro, M. Pegoraro, L. Posca, “Chemical modification of carbon fiber surfaces”, Carbon 2002;40:735-43.

[31] Z. Xu, Y. Huang, C. Zhang, G. Chen, “Influence of rare earth treatment on interfacial properties of carbon fiber/epoxy composites”, Mat. Sci. Eng. A 2007; 444:170-7.

[32] E. Pamula, P. G. Rouxhet, “Bulk and surface chemical functionalities of type III PAN-based carbon fibres”, Carbon 2003; 41:1905-13.

[33] S. Wang, Z. H. Chen, W. J. Ma, Q. S. Ma, “Influence of heat treatment on physical–chemical properties of PAN-based carbon fiber” Ceram. Int. 2006; 32:291-9.

[34] W. H. Lee, J. G. Lee, P. J. Reucroft, “XPS study of carbon fiber surfaces treated by thermal oxidation in a gas mixture of $O_2/(O_2+N_2)$”, Appl. Surf. Sci. 2001; 171:136-43.

[35] Qi Xiao, Shangjin He, Liwei Liu, Xianzhi Guo, Keyu Shi, Zongjie Du, Baolong Zhang, “Coating of multiwalled carbon nanotubes with crosslinked silicon-containing polymer”, Composites Science and Technology 68 (2008) 321–328.

[36] Yi Zheng Jin, Chao Gao, Harold W. Kroto,Toru Maekawa. Macromol. Rapid Commun, “Polymer-Grafted Carbon Spheres by Surface-Initiated Atom Transfer Radical Polymerization”, 2005, 26, 1133–1139, 2005 WILEY-VCH Verlag GmbH & Co. KGaA, Weinheim.

[37] Kuzmany. H, Kukovecz. A, Simon. F, Holzweber. M, Kramberger. Ch, Pichler. T. “Functionalization of carbon nanotubes”. Synth Metals 2004;141(1–2):113–22.

[38] Yu ZH, Brus LE, “Reversible oxidation effect in Raman scattering from metallic single-wall carbon nanotubes”, J Phys Chem 2000;A104:10995–9.

[39] Kuznetsova. A, Popova. I, Yates. JT, Bronikowski. MJ, Huffman. CB, Liu. J, et al. “Oxygen-containing functional groups on singlewall carbon nanotubes: NEXAFS and vibrational spectroscopic studies”, J Am Chem Soc 2001;123:10699–704.

[40] Kukovecz. A, Kramberger. C, Holzinger. M, Kuzmany. H, Schalko. J, Mannsberger. M, et al. “On the stacking behavior of functionalized single-wall carbon nanotubes”, J Phys Chem 2002;B106: 6374–6380.

[41] Mawhinney. DB, Naumenko. V, Kuznetsova. A, Yates. JT, Liu. J, Smalley. RE, “Surface defect site density on single walled carbon nanotubes by titration”, Chem Phys Lett 2000;324:213–6.

[42] Hu. H, Bhowmik. P, Zhao. B, Hamon. MA, Itkis. ME, Haddon. RC. “Determination of the acidic sites of purified single-walled carbon nanotubes by acid–base titration”, Chem Phys Lett 2001;345:25–8.

[43] Hao Kong, Chao Gao, and Deyue Yan, “Functionalization of Multiwalled Carbon Nanotubes by Atom Transfer Radical Polymerization and Defunctionalization of the Products”, Macromolecules 2004, *37,* 4022-4030

[43a] Hao Kong, Chao Gao, and Deyue Yan, “Controlled Functionalization of Multiwalled Carbon Nanotubes by in Situ Atom Transfer Radical Polymerization”.

[44] O'Connell, M. J, "Carbon nanotubes properties and applications", CRC Taylor & Francis: Boca Raton, (2006).

[45] Meyyappan. M, "Carbon nanotubes science and applications"; CRC Press: Boca Raton, FL, (2005).

[46] Harris. P. J. F, "Carbon nanotubes and related structures new materials for the twenty-first century"; Cambridge University Press: Cambridge, (2001).

[47] Weisenberger, M. C.; Grulke, E. A.; Jacques, D.; Rantell, T.; Andrews, R.; "Enhanced mechanical properties of polyacrylonitrile/multiwall carbon nanotube composite fibers", Journal of Nanoscience and Nanotechnology 3 (6), 535-539, **(2003)**.

[48] A. Fukunaga, S. Ueda, "Anodic surface oxidation for pitch-based carbon fibers and the interfacial bond strengths in epoxy matrices", Compos Sci Tech 2000;60:249-59.

[49] H. Cao, Y. Huang, Z. Zhang, J. Sun., "Uniform modification of carbon fibers surface in 3-D fabrics using intermittent electrochemical treatment", Compos Sci Tech 2005;65:1655-67.

[50] Baskaran. D, Mays. J. W, Bratcher. M. S, "Polymer adsorption in the grafting reactions of hydroxyl terminal polymers with multi-walled carbon nanotubes", Polymer 46 (14), 5050-5057, (2005).

[51] Ge. J. J, Zhang. D, Li. Q, Hou. H. Q, Graham. M. J, Dai. L. M, Harris. F. W, Cheng. S. Z. D, "Multiwalled carbon nanotubes with chemically grafted polyetherimides", Journal of the American Chemical Society 127 (28), 9984-9985, (2005).

[52] Liu. Y, Wu. D. C; Zhang. W. D, Jiang. X, He. C. B, Chung. T. S, Goh. S. H, Leong. K. W, "Polyethylenimine-grafted multiwalled carbon nanotubes for secure noncovalent immobilization and efficient delivery of DNA", Angewandte Chemie-International Edition 44 (30), 4782-4785, (2005).

[53] O'Connell. M. J, Boul. P, Ericson. L. M, Huffman. C, Wang. Y. H, Haroz. E, Kuper. C, Tour. J, Ausman. K. D, Smalley, R. E, "Reversible water-solubilization of single-walled carbon nanotubes by polymer wrapping", Chemical Physics Letters 342 (3-4), 265-271, (2001).

[54] Star. A, Stoddart. J. F, Steuerman. D, Diehl, M; Boukai. A, Wong. E. W, Yang. X, Chung. S. W, Choi. H, Heath. J. R, "Preparation and properties of polymer-wrapped single-walled carbon nanotubes", Angewandte Chemie-International Edition 40 (9), 1721-1725, (2001).

[55] Lou. X. D, Daussin. R, Cuenot. S, Duwez. A. S, Pagnoulle. C, Detrembleur. C, Bailly. C.Jerome. R, "Synthesis of pyrene-containing polymers and noncovalent sidewall functionalization of multiwalled carbon nanotubes", Chemistry of Materials 16 (21), 4005-4011, (2004).

[56] Chen. J, Liu. H. Y, Weimer, W. A, Halls. M. D, Waldeck. D. H, Walker. G. C, "Noncovalent engineering of carbon nanotube surfaces by rigid, functional conjugated polymers", Journal of the American Chemical Society 124 (31), 9034-9035, (2002).

[57] Ravindran. S, Chaudhary. S, Colburn. B, Ozkan. M; Ozkan. C. S, "Covalent coupling of quantum dots to multiwalled carbon nanotubes for electronic device applications", Nano Letters 3 (4), 447-453, (2003).

[58] Fumio Watari, Motohiro Uo, Tsukasa Akasaka, Iosif Daniel Rosca, "Oxidation of multiwalled carbon nanotubes by nitric acid ", Carbon 43 (2005) 3124–3131).

[59] Davis. K. A, Matyjaszewski. K, "Atom Transfer Radical Polymerization of *tert*-Butyl Acrylate and Preparation of Block Copolymers". Macromolecules 2000.

[60] Kuzmany. H, Kukovecz. A, Simon. F, Holzweber. M, Kramberger. Ch, Pichler. T, "Functionalization of carbon nanotubes", Synth Metals 2004;141 (1–2):113–22.

[61] Ajayan PM. Chem Rev1999;99:1787-1800.

[62] Shim M, Kam NWS, Chen RJ, Li Y, Dai H. Nano Lett 2002;2:285-288.

[63] Bianco A, Kostarelos K, Partidos C, Prato M. Chem Commun 2005:571-577.

[64] Lin Y, Meziani MJ, Sun YP. J Mater Chem 2007;17:1143-1148.

[65] Nanjundan Ashok Kumar, Hullathy Subban Ganapathy, Jong Su Kim, Yong Seok Jeong, Yeon Tae Jeong, "Preparation of poly 2-hydroxyethyl methacrylate functionalized carbon nanotubes as novel biomaterial nanocomposites".

[66] Yu ZH, Brus LE, "Reversible oxidation effect in Raman scattering from metallic single-wall carbon nanotubes", J Phys Chem 2000;A104:10995–9.

[67] Kuznetsova A, Popova I, Yates JT, Bronikowski MJ, Huffman CB, Liu J, et al., "Oxygen-containing functional groups on singlewall carbon nanotubes: NEXAFS and vibrational spectroscopic studies", J Am Chem Soc2001;123:10699–704 .

[68] Kukovecz A, Kramberger C, Holzinger M, Kuzmany H, Schalko J,Mannsberger M, et al. "On the stacking behavior of functionalized single-wall carbon nanotubes", J Phys Chem 2002; B106: 6374–6380.

[69] Mawhinney DB, Naumenko V, Kuznetsova A, Yates JT, Liu J,Smalley RE. "Surface defect site density on single walled carbon nanotubes by titration", Chem Phys Lett 2000;324:213–6.

[70] Hu H, Bhowmik P, Zhao B, Hamon MA, Itkis ME, Haddon C, "Determination of the acidic sites of purified single-walled carbon nanotubes by acid–base titration", Chem Phys Lett 2001;345:25–8.

[71] Riggs JE, Guo ZX, Carroll DL, Sun YP. J Am Chem Soc 2000;122:5879-5880.

[72] Lin Y, Rao AM, Sadanadan B, Kenik EA, Sun Y. J Phys Chem B 2002;106:1294-1298

[73] Fumio Watari, Motohiro Uo, Tsukasa Akasaka, Iosif Daniel Rosca, "Oxidation of multiwalled carbon nanotubes by nitric acid ", Carbon 43 (2005) 3124–3131).

[73a] Qiao Chen , Riwei Xu, Dingsheng Yu , "Multiwalled carbon nanotube/polybenzoxazine nanocomposites: Preparation, characterization and properties", Polymer 47 (2006) 7711& 7719.

[74] Chao Gao, Cong Duan Vo,Yi Zheng Jin, Wenwen Li, and Steven P. Armes, "Multihydroxy Polymer-Functionalized Carbon Nanotubes: Synthesis, Derivatization, and Metal Loading", Macromolecules 2005**,** 38, 8634-8648.

[74a] Hesheng Xia, Mo Song, Jie Jin, Lei Chen .Macromol, "Poly(propylene glycol)-Grafted Multi-Walled Carbon Nanotube Polyurethane", Chem. Phys. 2006, 207, 1945–1952.

[74 b] Marcos Gomes Ghislandi, "Functionalization of carbon nanofibers surface via acid / peroxide oxidation, anchoring of a diol spacer and acrylate polymerization. [MSc thesis] ", Technische Universität Hamburg-Harburg (Germany), 2007.

[75] J. Zhang, H. Zou, Q. Qing, Y. Yang, Q. Li, Z. Liu, X. Guo, Z. Du, J. Phys. Chem. B 2003, 107, 3712.

[76] Halasa, A. F. *Rubber Chemistry Technology*, 1981.

[77] Webster, *O. W. Science*, 1991.

[78] Wikimedia Foundation, Inc., a US-registered nonprofit charity http://www.wikipedia.com 10.03.2007

[79] S. Edmondson, V.L. Osborne, W.T.S. Huck, Chem. Soc. Rev. 33 (2004) 14.

[80] S. Palacin, C. Bureau, J. Charlier, G. Deniau, B. Mouanda, P. Viel, Chem. Phys. Chem. 5 (2004) 1468.

[81] E.P.K. Currie, W. Norde, M.A. Cohen Stuart, Adv. Colloid Interface Sci. 100–102 (2003) 205.

[82] K.Matyjaszewski, J. Xia, Chem. Rev. 101 (2001) 2921.

[83] K. Matyjaszewski, S. Qin, J.R. Boyce, D. Shirvanyants, S.S. Sheiko, Macromolecules 36 (2003) 1843.

[84] Hao Kong, Ping Luo, Chao Gao, "Polyelectrolyte functionalised multiwalled carbon nanotubes preparation, characterization and layer-by-layer self-assembly".

[85] A. Fukunaga, T. Komami, S. Ueda, M. Nagumo, "Plasma treatment of pitch-based ultra high modulus carbon fibers", Carbon 1999;37:1087-92.

[86] A.P. Kettle, A.J. Beck, L.O. Toole, F.R. Jones, "Plasma polymerisation for molecular engineering of carbon-fibre surfaces for optimised composites", Compos. Sci. Tech. 1997; 57:1023-30.

[87] M. A. Montes-Moran, A. Martinez-Alonso, J. M. Tascon, "Effects of plasma oxidation on the surface and interfacial properties of ultra-high modulus carbon fibres", Compos Part A 2001;32:361-6.

[88] J. P. Boudou, J. I. Paredes, A. Cuesta, A. Martinez-Alonso, "Oxygen plasma modification of pitch-based isotropic carbon fibres", Carbon 2003;41:41-8.

[89] F. Severini, L. Formaro, M. Pegoraro, L. Posca., "Chemical modification of carbon fiber surfaces ", Carbon 2002;40:735-43.

[90] Z. Xu, Y. Huang, C. Zhang, G. Chen., "Influence of rare earth treatment on interfacial properties of carbon fiber/epoxy composites", Mater Sci Eng A 2007; 444:170-7.

[91] E. Pamula, P. G. Rouxhet., "Bulk and surface chemical functionalities of type III PAN-based carbon fibres", Carbon 2003; 41:1905-13.

[92] S. Wang, Z. H. Chen, W. J. Ma, Q. S. Ma., "Influence of heat treatment on physical–chemical properties of PAN-based carbon fiber",. Ceram Int 2006;32:291-9.

[93] W. H. Lee, J. G. Lee, P. J. Reucroft. "XPS study of carbon fiber surfaces treated by thermal oxidation in a gas mixture of O2/(O2+N2) ", Appl Surf Sci 2001; 171:136-43.

[94] Burakowski L. Estudo da interface de compósitos termoplásticos estruturais processados a partir de fibras de carbono com superfícies modificadas. [MSc thesis]. Instituto Tecnológico de Aeronáutica; São José dos Campos; 2001.

[95] Burakowski L, Rezende MC. Modificação da rugosidade de fibras de carbono por método químico para aplicação em compósitos poliméricos. Polímeros: Ciência e Tecnologia. 2001; 11(2):51-57.

[96] Zielke U, Hüttinger KJ, Hoffman WP. Surface-oxidized carbon fibers: I. surface structure and chemistry. Carbon. 1996; 34(8):983-998.

[97] Pittman Jr. CU, He GR, Wu B, Gardner SD., "Chemical modification of carbon fiber surfaces by nitric acid oxidation followed by reaction with tetraethylenepentamine ", Carbon. 1997; 35(3):317-331.

[98] Hull D, Clyne TW., "An introduction to composite materials", 2nd edition. Melbourne: Cambridge University Press; 1996.

[99] Fujimaki H, et al., "Process for the surface treatment of carbon fibers", U.S. patent. 4,009,305, 1977.

[100] Yue ZR, Jiang W, Wang L, Gardner SD, Pittman Jr. CU. ," Surface characterization of eletrochemically oxidized carbon fibers", Carbon. 1999; 37(11):1785-1796.

[101] Liliana Burakowski Noharaa, Gilberto Petraconi Filhob, Evandro Luís Noharac, “Evaluation of Carbon Fiber Surface Treated by Chemical and Cold Plasma Processes”, Materials Research, Vol. 8, No. 3, 281-286, 2005

[102] K.J. Sanders, Organic Polymer Chemistry, Chapman & Hall, (1 988). 4 12-436.

[103] F.W. Billmeyer, Text Book Of Polymer Science, Jhon Wiley & Sons Inc.. (1984) 3-4, 436-446

[104] Tripathi, D. Jones, F.R, “Review: Single fiber fragmentation test for assessing adhesion in fiber reinforced composites”,J.Mat.Sci.33, 1998, pp.1-16.

[105] Schjodt-Thomsen,J.,” A micro Raman investigation of viscoelasticity in short fiber reinforced polymer matrix composites”, Ph.D. Dissertation, Aalborg University, January 2000, ISSN0905-2305.

[106]. E.Klinklin, M.Guigon, " Characterization of the Interface and Interphase in Carbon on Fiber Reinforced Composites", 83-85.

[107] A.P. Kettle, A.J. Beck, "Plasma Polymerization For Molecular Engineering of Carbon-Fiber Surfaces For Optimized Composites, Composites Science And Technology", VOL. 57 NO. 8, (1 997), 1023-1024.

[108] Y. SAWADA, Y. NAKANISHI and T. FUKUDA “Effect of carbon fibre surface on interfacial adhesive strengths in CFRP” (Government Industrial Research Institute of Osaka/"Osaka City University, Japan).

[109] Zhang, H., Zhang,Z., Breidt, C., “ Comparison of short carbon fiber surface treatments on epoxy composites I. Enhancement of the mechnical properties”, Comp.Sci.Tech. 64, 2003, pp 2021-2029.

[110] Nielsen, A.S., “ Micromechanical modeling of thermal stress in polymeric matrix composites based on raman microscopy”, Ph.D- Thesis, Institute of Mechanical Engineering Aalborg University, 2000. ISSN 0909-2305.

[111] Wartewig, S., "IR and Raman spectroscopy: fundamental processing”, Wiley-VCH, 2003.

[112] Weber, W.H., Merlin, R.,“ Raman scaterring in material scienve“., Springer-Verlag Berlin,2000.

[113] Galiotis,C., Batchelder, D.N.,“ Strain dependences of the first-and second-order Raman spectra of carbon fibers” ,J. Mat. Sci. letters 7, 1998, pp. 545-547.

[114] Paipetis and C Galiotis, “Effect of fiber sizing on the stress transfer efficiency in carbon/epoxy model composites”, Comp, part A 27A, 1996, pp.755-767.

[115] Young,R.J., “Monitoring Deformation Process in high-performance fibers using Raman spectroscopy”, J. text.Inst., 1995,86 No.2, pp.360-381.

[116] Guild, F.J., Vlattas, C., Galiotis., C., “Modeling of stress transfer in fiber composites” Comp. Sci. Tech. 50,1994, pp. 319-322.

[117] Paipetis and C Galiotis, “Modelling the stress-transfer efficiency of carbon-epoxy interfaces”, Proc. R. Soc. Land. A, 2001,457, pp. 1555-1577.

[118] Sanwat N. Chaudhuri , Reaz A. Chaudhuri , Robert E. Benner , Madhu S. Penugonda, “Raman spectroscopy for characterization of interfacial debonds between carbon fibers and polymer matrices”. Composite Structures 76 (2006) 375–387, pp. 376-379.

[119] Marston. C, Gabbitas. B., Adams, J., Marshall, P., Galiotis C, “Measurement of stress concentration around fiber breaks in carbon-fiber/epoxy-resin composite tows”, Comp. Sci. Tech 57, 1997, pp. 913-923.

[120] Galiotis, C., “A study of mechanisms of stress transfer in continuous- and discontinuous-fiber model composites by laser Raman spectroscopy”, Comp. Sci. Tech. 48,1993, pp.15-28.

[121] L.S. Schalder, “Fundamentals and applications of micro Raman spectroscopy to strain measurements in fiber reinforced composites”, International material Reviews 1995 Vol.40 no.3 PP.127-129.

[121a] L.R Jensen, J.C Rauhe and R.Pyrz. (2007), “Presentation on interfacial properties of carbon fiber-epoxy composites under fatigue loading”, 28th Riso International Symposium on Materials Science, Riso, Denmark. September 3-6,2007.

[122] http://en.wikipedia.org/wiki/Image:CNTnames.png

[123] http://www.nanotubes.com.cn

[124] http://students.chem.tue.nl/ifp03/images/mwnt.gif

[125] http://en.wikipedia.org/wiki/Image:CNTnames.png

[126] Erlangung des Doktorgrades, “Carbon nanotube composites - mechanical, electrical and optical properties”. Dissertation, Universität Bonn, 2006.

[127] http://www.nanotubes.com.cn/specification.htm

[128] http://en.wikipedia.org/wiki/Raman_scattering

[129] http://en.wikipedia.org/wiki/Raman_spectroscopy

[130] http://www.quantiki.org/wiki/index.php/Raman_transitions

[131] Shiv K. Sharma, Anupam K. Misra, Bhavna Sharma, “Portable remote Raman system for monitoring hydrocarbon, gas hydrates and explosives in the environment”, Spectrochimica Acta Part A: Molecular and Biomolecular Spectroscopy Volume 61, Issue 10, August2005, Pages 2404-2412.

[132] Nataliya Kalashnyk, Orkey Milagres Ferri, “ Influence of fiber sizing on interface properties of carbon/epoxy composites”, project work report, Aalborg University, Denmark, 2005.

[133] Wong, E. W, Sheehan, P. E, Lieber, C. M, "Nanobeam mechanics: Elasticity, strength, and toughness of nanorods and nanotubes", Science 277 (5334), 1971-1975, **(1997)**.

[134] Lau. K. T, Hui. D, "The revolutionary creation of new advanced materials - carbon nanotube composites", Composites Part B-Engineering 33 (4), 263-277, **(2002)**.

[135] Li. F, Cheng. H. M, Bai. S, Su. G, Dresselhaus. M. S, "Tensile strength of single-walled carbon nanotubes directly measured from their macroscopic ropes", Applied Physics Letters 77 (20), 3161- 3163, **(2000)**.

[136] Iijima. S, Brabec, C. Maiti. A, Bernholc. J, "Structural flexibility of carbon nanotubes", Journal of Chemical Physics 104 (5), 2089-2092, (**1996).**

[136 (a)]

[137] http://en.wikipedia.org/wiki/Carbon_nanotube

[138] Hiren Wang, “ Functionalization of Carbon Nanotubes: Characterization, Modeling and Composite Applications”, PhD dissertation, Department of Industrial and Manufacturing Engineering, Florida state university, 2006.

[139] Lau, K. T, Hui, D, "The revolutionary creation of new advanced materials - carbon nanotube composites", Composites Part B-Engineering 33 (4), 263-277, **(2002)**.

[140] O'Connell, M. J, "Carbon nanotubes properties and applications", CRC Taylor & Francis: Boca Raton, **(2006)**.

[141] Minami. N, Kazaoui. S, Jacquemin. R, Yamawaki. H, Aoki. K, Kataura. H, Achiba. Y, "Optical properties of semiconducting and metallic single wall carbon nanotubes: effects of doping and high pressure", Synthetic Metals 116 (1-3), 405-409, **(2001)**.

Annex-1

FTIR spectrum of PtBA

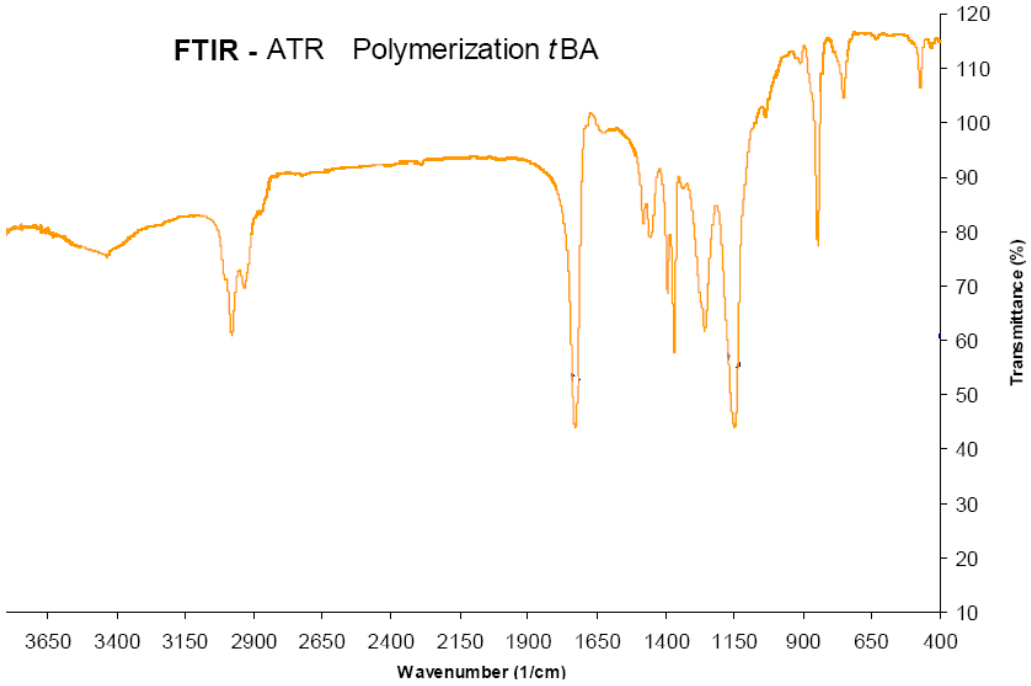

Annex-2

Stree strain curve for the tensile test of modified CF/epoxy composite